

Regenerative neurogenesis is induced from glia by Ia-2 driven neuron-glia communication

Neale Harrison^{1,2*}, Elizabeth Connolly^{1*}, Alicia Gascón Gubieda^{1,3}, Zidan Yang^{1,4}, Benjamin Altenhein⁵,
Maria Losada-Perez⁶, Marta Moreira¹ and Alicia Hidalgo^{1#}

* These authors contributed equally

1, NeuroDevelopment Group, School of Biosciences, University of Birmingham, UK. 2, Current address: Tomlinson Lab, School of Biosciences, University of Birmingham, UK. 3, Current address: Institute for Cell and Molecular Biosciences, Newcastle University, Newcastle upon Tyne NE2 4HH, UK. 4, Current address: Max Planck Florida Institute for Neuroscience, 1 Max Planck Way, Jupiter, Florida 33458, USA; 5, Institute of Zoology, University of Cologne, Germany; 6, Instituto Cajal, Consejo Superior de Investigaciones Científicas (CSIC), Madrid, Spain.

Author for correspondence:

Professor Alicia Hidalgo ph 00 44 (0)121 4145416 a.hidalgo@bham.ac.uk

Word count: 6,711 in main text

Figures: 8 main figures, plus 4 supplementary figures.

Keywords: Drosophila, CNS, neuron, glia, neural stem cell, regeneration, kon-tiki, NG2, insulin, ia-2, prospero, Notch, Deadpan, Repo, glial regenerative response, neurogenesis, damage, injury, spinal cord, brain, ventral nerve cord, larva.

ABSTRACT

A key goal to promote central nervous system regeneration is to discover mechanisms of injury-induced de novo neurogenesis. Glial cells might induce neurogenesis upon injury, but this is debated, and underlying mechanisms are unknown. A critical missing link is the identification of neuronal factors that could interact with glial NG2 to facilitate regeneration. Here, we used *Drosophila* genetics to search for neuronal partners of the NG2 homologue Kon-tiki (Kon), and identified Ia-2, involved in insulin secretion. Ia-2 is exclusively neuronal, and alterations in Ia-2 function destabilized cell fate. Injury increased *ia-2* expression and induced neural stem cells. Using glial markers, genetic epistasis analysis and lineage tracing, we demonstrate that Ia-2 functions together with Kon and Dilp6 to induce de novo neural stem cells from glia. Altogether, Ia-2 and Kon initiate a neuron-glia interaction loop that coordinates de novo production of both neurons and glia for central nervous system regeneration.

INTRODUCTION

Humans cannot regenerate the central nervous system (CNS) after injury, but some animals do and regeneration most often involves de novo neurogenesis (Tanaka and Ferretti, 2009). Thereafter, newly formed neurons integrate into functional neural circuits. This enables the recovery of function and behavior, which is how CNS regeneration is measured (Tanaka and Ferretti, 2009). The brains of humans and most vertebrates continue to produce new neurons in response to the environment throughout life, they also integrate into functional circuits, and this constitutes one of the key manifestations of structural brain plasticity (Gage, 2019; Tanaka and Ferretti, 2009). Thus, even the adult human brain has cells that can respond to environmental challenge. If we could understand the molecular mechanisms underlying natural regenerative neurogenesis, we would be able to further enhance de novo neurogenesis to promote regeneration in the human CNS, after damage or disease. The fact that regenerative neurogenesis is found in many diverse animals may reflect an ancestral, evolutionarily conserved genetic mechanism, which manifests itself to various degrees in fully

regenerating and non-regenerating animals (Tanaka and Ferretti, 2009). On this basis, it may be possible to discover molecular mechanisms of injury-induced neurogenesis in the fruit-fly *Drosophila*, which is the most powerful genetic model organism.

Regenerative neurogenesis could occur through either activation of quiescent neural stem cells, de-differentiation of neurons or glia, or direct conversion of glia to neurons. Across many regenerating animals, new neurons originate mostly from glial cells (Falk and Gotz, 2017; Tanaka and Ferretti, 2009). Thus, unravelling the molecular mechanisms that switch glial cells into becoming neural stem cells or neurons is of paramount importance. In the mammalian CNS, glial cells can often behave like neural stem cells, even in normal development (Falk and Gotz, 2017). For instance, radial glia normally produce neurons during development, and in the adult brain, new neurons are produced daily in the hippocampus from these glial cells (Falk and Gotz, 2017). There is evidence that in the mammalian CNS, astrocytes and NG2-glia (also known as oligodendrocyte progenitor cells, OPCs), can produce neurons, most particularly upon injury (Dimou and Gotz, 2014; Falk and Gotz, 2017; Valny, et al., 2017; Vigano and Dimou, 2016). NG2-glia are most relevant, as they are the only progenitor cell type in the adult brain, constitute 5-10% of cells in the total human CNS and remain proliferative throughout life (Dimou and Gotz, 2014). In the normal intact CNS, NG2-glia are progenitors of astrocytes, OPCs and oligodendrocytes, and upon injury they can also produce neurons (Dimou and Gotz, 2014; Torper, et al., 2015; Valny, et al., 2017). They can also be directly reprogrammed into neurons that integrate into functional circuits (Pereira, et al., 2017; Torper, et al., 2015). The functions and diversity of NG2-glia are not yet fully understood, but they are particularly close to neurons: they receive and respond to action potentials integrating them into calcium signaling, they survey and modulate the state of neural circuits by regulating channels, secreting chondroitin sulfate proteoglycan perineural nets, and inducing their own proliferation to generate more NG2 glia, astrocytes that sustain neuronal physiology, and oligodendrocytes that enwrap axons (Dimou and Gotz, 2014; Sakry and Trotter, 2016; Sun, et al., 2016). To what extent these functions depend on the *NG2* gene and protein, is not known.

In the CNS, NG2 is expressed by NG2-glia and pericytes, but not by oligodendrocytes, neurons, or astrocytes. NG2 is a large transmembrane protein that can be cleaved upon neuronal stimulation by α - and γ -secretases, to release secreted and intra-cellular forms (Sakry, et al., 2014; Sakry and Trotter, 2016). The intracellular domain (ICD) - NG2^{ICD} - is mostly cytoplasmic, and it activates protein translation and induces cell cycle progression (Nayak, et al., 2018). NG2^{ICD} lacks a DNA binding domain and therefore does not directly function as a transcription factor, but it has a nuclear WW4 domain, nuclear localization signals, it was found in the nucleus and can regulate gene expression (Nayak, et al., 2018; Sakry and Trotter, 2016; Sakry, et al., 2015). NG2 is abundant in proliferating NG2-glia and glioma (Nayak, et al., 2018; Sakry and Trotter, 2016; Sakry, et al., 2015). NG2 is required for OPC proliferation and migration in development and in response to injury, and it participates in glial scar formation (Biname, et al., 2013; Kucharova, et al., 2011; Kucharova and Stallcup, 2010). Potentially, NG2 may endow OPCs with plastic, homeostatic and repair properties in interaction with neurons (Dimou and Gotz, 2014; Sakry and Trotter, 2016). However, whether NG2 itself may be involved in de novo neurogenesis remains unresolved. A critical missing link is the identification of neuronal partners that might interact with NG2 to induce regenerative neurogenesis.

The fruit-fly *Drosophila* is particularly powerful for identifying novel molecular mechanisms. The *Drosophila* NG2 homologue is called *kon-tiki* (*kon*) or *perdido* (Perez-Moreno, et al., 2017; Schnorrer, et al., 2007). Kon promotes glial proliferation and cell fate determination in development and upon injury (Losada-Perez, et al., 2016). Kon works in concert with Notch and Prospero (Pros) to drive the glial regenerative response to CNS injury (Kato, et al., 2011; Losada-Perez, et al., 2016). Notch signaling activates *kon* expression, and together they promote glial proliferation; Kon is also essential to determine neuropile glial cell fate, which ultimately depends on Pros; and Pros inhibits glial proliferation, inhibits *kon* expression and maintains glial cell differentiation (Griffiths and Hidalgo, 2004; Kato, et al., 2011; Losada-Perez, et al., 2016). Thus, Notch and Kon promote neuropile glial proliferation, and Pros their differentiation. The relationship

between these genes is also conserved in the mouse, where the homologue of *pros*, *prox1*, is critical for oligodendrocyte differentiation (Kato, et al., 2015). Together, Notch, Kon and Pros form a homeostatic gene network that sustains neuropile glial integrity throughout the life-course and drives glial regeneration upon injury (Hidalgo and Logan, 2017;Kato, et al., 2018).

Remarkably, we noticed that injury to the *Drosophila* larval CNS resulted in spontaneous, yet incomplete, repair also of the axonal neuropile (Kato, et al., 2011). This strongly suggested that injury might also induce improvements in neurons. These could correspond to axonal regrowth, or generation of new neurons. Here, we asked whether Kon may interact with neuronal partners that could contribute to regenerative neurogenesis after injury.

RESULTS

la-2 is a functional partner of Kon expressed in neurons

Genetic manipulation of glia induced axonal neuropile repair, and up-regulation of *kon* in glia was sufficient to induce CNS repair (Kato, et al., 2011;Losada-Perez, et al., 2016), implying that Kon might interact with neuronal factors during regeneration. To search for neuronal partners of Kon, we carried out genetic screens that aimed to identify genes expressed in neurons with non-autonomous effects on glia. We tested whether RNAi knock-down of candidate genes in neurons or glia rescued the extended ventral nerve cord phenotype of over-expressed full-length *kon* (Supplementary Figures S1 and S2). We tested factors predicted or known to interact with Kon and/or NG2 (Perez-Moreno, et al., 2017;Schnorrer, et al., 2007), and factors involved in Notch signaling, to validate the approach; phosphatases, as a relationship of Kon/NG2 had previously been reported for Prl1 and Ptp99A (Song, et al., 2012); and other transmembrane proteins expressed in neurons. Rescue by knock-down of known interactors, such as *integrins* (Perez-Moreno, et al., 2017), factors involved in Notch signaling (e.g. *Mtm*, *Akap200*), secretases (i.e. *kuz*, *kuz-I*) that cleave both Notch and NG2/Kon (Sakry and Trotter, 2016) and *prl-1* (Song, et al., 2012), validated the approach (Supplementary Figure 1A-F). Amongst the novel hits, most prominent were genes encoding transmembrane protein

phosphatases and insulin-related factors, including phosphatase *LAR*, *Akt* and phosphatase-dead *ia-2* (Supplementary Figure 2A-D). Ptp2A negatively regulates insulin receptor signaling, maintaining neural stem cell quiescence (Gil-Ranedo, et al., 2019). *LAR* is involved in neuronal axon guidance, and is responsible for de-phosphorylating, and thus inactivating, insulin receptor signaling (Mooney, et al., 1997;Wills, et al., 1999). *Akt* is a key effector of insulin receptor signalling downstream (Van Der Heide, et al., 2006). *ia-2* is a highly evolutionarily conserved phosphatase-dead transmembrane protein phosphatase required in dense core vesicles for the secretion of insulin, insulin-related factor-1 (IGF-1) and neurotransmitters. It also has synaptic functions and influences behaviour and learning (Cai, et al., 2009;Cai, et al., 2011;Cai, et al., 2001;Carmona, et al., 2014;Harashima, et al., 2005;Henquin, et al., 2008;Hu, et al., 2005;Nishimura, et al., 2010).

Kon is required in glia, it influences gene expression, and loss of *kon* function prevents expression of glial differentiation markers (Losada-Perez, et al., 2016). Thus, to further test the functional relationship to *kon*, we used quantitative real-time reverse transcription PCR (qRT-PCR) on dissected larval CNS, to ask whether *kon* loss or gain of function affected the expression of genes identified from the genetic screens. Consistently, *kon* knock-down in neurons (with *kon*^{c452}, *elavGAL4>UAS-konRNAi*) had no effect, whereas in glia (with *kon*^{c452}, *repoGAL4>UAS-konRNAi*) it resulted in a 3-fold increase in *ia-2* mRNA levels (Supplementary Figure 3A). Conversely, over-expression of full-length *kon* in either neurons or glia down-regulated *ia-2* mRNA levels by 25% (Supplementary Figure 3B). We validated these results by increasing the repeats of the most promising subset of genes (Supplementary Figure 3C,D), and this confirmed the strongest effect of *kon* loss and gain of function on *ia-2* mRNA levels (Figure 1A). This data showed that *Kon* prevents *ia-2* expression. Next, we asked whether knock-down or over-expression of *ia-2* in neurons (with *elavGAL4*) had any effect on *kon* mRNA levels, but none did (Figure 1B). However, over-expression of *ia-2* in glia (with *repoGAL4>ia-2[GS11438]*) decreased *kon* mRNA levels (Figure 1B). These data indicate that *Kon* and *ia-2* restrict each other's expression to glia or neurons, respectively. Since both

Kon and Ia-2 are transmembrane proteins, this effect is presumably indirect. Together, these data identified Ia-2 as a factor that interacts genetically with Kon.

Kon functions in concert with Notch and Pros during glial regeneration (Kato, et al., 2011; Losada-Perez, et al., 2016). Thus, to ask how *ia-2* might relate to this regenerative gene network, we tested whether loss or gain of function of *pros* or *Notch* might affect the expression levels of *ia-2* in dissected larval CNSs. *Notch^{ts}* mutants caused an almost two-fold increase in *ia-2* expression, whereas *Notch^{ICD}* over-expression in glia (*repoGAL4>Notch^{ICD}*) caused a mild downregulation of *ia-2* (Figure 1C). So, Notch prevents *ia-2* expression in glia. This resembles the effect of *kon* on *ia-2*, consistently with the fact that *kon* depends on *Notch* (Losada-Perez, et al., 2016). *ia-2* mRNA levels also increased in *pros* mutant larvae, but mostly when *pros* was over-expressed in glia (Figure 1D). The loss of function phenotype is most likely indirect, as in glial cells Pros and Notch depend on each other (Kato, et al., 2011), so loss of *pros* causes the down-regulation of *Notch*, which would increase *ia-2* expression. Instead, the stronger effect of *pros* gain of function on *ia-2*, and the fact that Pros is a transcription factor, indicate that Pros may directly regulate *ia-2* expression. Importantly, *pros* is expressed, as well as in glia, in all ganglion mother cells and some neurons, raising the possibility that Pros may activate *ia-2* expression during a cell-fate transition. Altogether, these data show that *ia-2* expression is repressed by *kon* and *Notch* in glia, and activated by *pros*. These data mean that *ia-2* is functionally related to the *kon*, *Notch*, *pros* gene network that drives the regenerative response to CNS injury.

The above data suggested that *ia-2* expression is normally repressed in glia. To test what cells normally express *ia-2*, we knocked-down *ia-2* with RNAi in either neurons or glia and measured *ia-2* mRNA levels with qRT-PCR in dissected larval CNSs. *ia-2-RNAi* knock-down in glia (with *repoGAL4*) did not affect mRNA levels compared to wild-type, however knock-down in neurons (with *elavGAL4*) down-regulated *ia-2* transcripts to about 20% of wild-type levels, showing that *ia-2* is expressed in neurons (Figure 1E). To visualize *ia-2* expression in vivo, we used a transgenic protein fusion of Ia-2 to yellow fluorescent protein (YFP). Ia-2YFP+ cells did not have the glial marker anti-

Repo, nor anti-Deadpan (Dpn), which is the general neuroblast marker and also labels transit amplifying ganglion mother cells in type II neuroblast lineages (Boone and Doe, 2008), but all Ia-2YFP+ cells were Elav+ (Figure 1G,H,J). This demonstrates that *ia-2* is expressed exclusively in neurons.

Altogether, these data show that Ia-2 and Kon are restricted to neurons and glia, respectively (Figure 1F), and that Ia-2 is a functional neuronal partner of Kon.

Ia-2 can regulate neurogenesis

Next, we carried out a functional analysis of *ia-2* in the CNS. As *kon* knock-down increased *ia-2* mRNA levels, we sought to verify this using Ia-2-YFP. We found that *kon* loss of function in glia (*kon*^{c452}/+; *repoGAL4>kon-RNAi*) increased the number of Ia-2-YFP+ cells along the midline (Figure 2A,B). The ectopic cells did not have the glial marker Repo (Figure 2C). Midline cells were unaffected by *kon* over-expression in either neurons or glia (Figure 2A,B, *elavGAL4>kon* and *repoGAL4>kon*). Thus, in the absence of *kon*, ectopic Ia-2-YFP+ neurons were found at the midline. These results could also partly explain the increased *ia-2* mRNA levels seen with *kon* loss of function.

To ask what function *ia-2* might have in neurons, we altered *ia-2* expression and visualized the effect using standard neuronal markers. *ia-2* knock-down in neurons (*elavGAL4>ia-2RNAi*) had no obvious detectable effect on FasII or BP102 (Supplementary Figure 4A,B), and it did not change Eve+ neuron number either (Figure 2D,E). As Pros activates *ia-2* (Figure 1D), we asked whether *ia-2* might in turn affect Pros. Over-expression of *ia-2* in either neurons or glia had no effect on Pros+ cells (Figure 2F,G). By contrast, *ia-2* knock-down in neurons (*elavGAL4>ia-2RNAi*) increased Pros+ cell number, and these cells looked small (Figure 2F,G). Pros is normally found in neuropile glia, some neurons and all ganglion mother cells, suggesting that ectopic Pros+ cells might be ganglion mother cells or neurons, which are generally smaller than glia.

To test whether ectopic Pros+ cells originated from neural stem cells, we asked whether altering *ia-2* function might affect the expression of *deadpan* (*dpn*), a general neuroblast marker.

Both *ia-2* gain of function (*elav>ia-2*) and loss of function (*Df(2L)ED7733/+; elav>ia-2RNAi*) in neurons increased the number of abdominal VNC Dpn+ cells (Figure 2H,I,J). The increase in Dpn+ cell number also correlated with tumorous overgrowths in the VNC (Figure 2H), characteristic of genotypes causing ectopic neuroblast proliferation. The ectopic Dpn+ cells included cells along the midline, and cells surrounding the neuropile, in positions normally occupied by glial cells (Figure 2I). The ectopic Dpn+ cells were distinct from normal larval neural stem cells, which are ventro-lateral and further from the neuropile. Furthermore, they were visualised at 120h after egg laying (AEL), after the normal disappearance of normal abdominal neural stem cells. Thus, alterations in the normal levels of neuronal *ia-2* induced neuroblast marker expression ectopically.

These data showed that interference with normal neuronal *ia-2* levels destabilizes cell fate, and induces ganglion mother cell and neural stem cell markers. This effect appeared to be non-autonomous, as neurons themselves were unaffected. As *ia-2* and *Kon* are functionally related and confined to either neurons or glia, respectively, this suggested that communication between neurons and glia might modulate cell fate stability.

Injury up-regulates *ia-2* expression and induces regenerative neurogenesis

Data had shown that altering normal *ia-2* levels induced expression of the neural stem cell marker Dpn. CNS injury induced the up-regulation of *kon* expression (Losada-Perez, et al., 2016). Thus, we asked whether injury might affect *ia-2* expression and, consequently, induce neurogenesis. Crush injury was carried out at 74-76h after egg laying (AEL) in early third-instar larval VNCs labelled with the endoplasmic reticulum GFP marker G9 (Figure 3A). qRT-PCR in injured VNCs revealed a virtually 2-fold increase in *ia-2* mRNA levels at 5-7h post-injury, which recovered homeostatically by 24h post-injury (Figure 3C). Thus, CNS injury caused an increase in *ia-2* expression.

Since increased *ia-2* levels induced ectopic Dpn+ cells (Figure 2I,J), and *ia-2* was up-regulated in injury, we asked whether injury induced neurogenesis. We focused in the abdominal VNC only, which has 3 neuroblasts per hemi-segment in the early third instar larva, that occupy ventro-lateral

positions. Crush injury in the abdominal VNC at 74-76h AEL resulted in ectopic Dpn+ cells by 5-7h later (Figure 3A,B,D, in n=6/17 VNCs). These were more numerous than the normal developmental abdominal larval neuroblasts, and included cells located in dorsal positions not normally taken by them (Figure 3B,D; see (Froldi, et al., 2015; Sousa-Nunes, et al., 2011)). The numerous Dpn+ cells could correspond to injury-induced divisions of neuroblasts normally found during larval development. To test whether injury might induce ectopic neural stem cells distinct from developmental neuroblasts, we next carried out crush injury at three later time points (Figure 3E,F): (1) at 96h AEL and analysed the VNCs 6 post-injury (PI, 102h AEL), when in control VNCs, abdominal hemi-segments have 0 or 1 Dpn+ cell remaining. (2) At 105h and analysed 24h PI (129h AEL), when in controls there are no ventro-lateral neuroblasts, only Dpn+ cells along the midline; and (3) at 117h AEL and analysed the VNCs 12h post-injury (129h AEL), taking also advantage of the delayed pupariation of injured larvae. At 129h AEL there are no remaining abdominal ventro-lateral neural stem cells in intact controls, only some Dpn+ cells along the midline (Figure 3I). Injury induced at these three time points, caused ectopic Dpn+ cells compared to controls (Figure 3G-J, Ectopic Dpn+ cells in abdominal VNC: Injury 96h AEL, analysis 6h PI (102h AEL) in n=4/9 VNCs; injury at 105, analysis at 24h PI in n=2/11 VNCs; Injury 117h AEL, analysis 12h PI (129h AEL) in n=9/32). Most but not all ectopic Dpn+ cells lacked *la-2*YFP. Importantly, most ectopic Dpn+ cells surrounded the neuropile, and some were dorsal, in positions never occupied by developmental neural stem cells (Figure 3H,J). These data show that injury induces ectopic neural stem cells. Since *ia-2* levels increased upon injury, and *ia-2* gain of function induced neural stem cells, this suggested that *ia-2* was responsible for the increase in Dpn+ cells caused by injury.

These data raised the question of how might *ia-2* induce neurogenesis.

Dilp6 depends on neuronal *la-2* and glial Kon

la-2 is highly conserved and it functions in dense core vesicles to release insulin and neurotransmitters (Cai, et al., 2011; Harashima, et al., 2005; Kim, et al., 2008; Nishimura, et al., 2010).

There are eight *Drosophila* insulin-like-peptides (Dilps) and *ia-2* affects only Dilp-6 (Kim, et al., 2008). *dilp-6* is expressed in cortex and blood brain barrier CNS glia, and activates neuroblast proliferation following a period of quiescence in normal larval development (Chell and Brand, 2010; Sousa-Nunes, et al., 2011). Thus, we asked whether the increase in Dpn+ cells in *ia-2* loss and gain function observed above involved *dilp-6*. We visualized *dilp-6* expressing cells in wandering larvae using *dilp6-GAL4* (Chell and Brand, 2010; Sousa-Nunes, et al., 2011) to drive expression of the nuclear reporter Histone YFP. Most *dilp-6>YFP+* cells were also Repo+, but they did not surround the neuropile and lacked the neuropile glial marker Pros (Figure 4A,B). Thus, most *dilp-6* expressing cells in the abdominal larval VNC were cortex and surface glia, as previously reported (Chell and Brand, 2010; Sousa-Nunes, et al., 2011). Some *dilp6>his-YFP+* cells were Repo-negative and Elav+, and thus were neurons (Figure 4A,B). Thus, *dilp-6* is expressed in a few neurons per VNC segment, and mostly in non-neuropile glia.

To ask what cells might receive Dilp6, we visualized the expression of its receptor, the *insulin receptor (InR)*, using an available GAL4 line, *InR^{NP2552}*, to drive histone-YFP, and tested co-localisation with glial and neuronal markers. *InR^{NP2552}>his-YFP+* cells were mostly Repo+ neuropile glia and a few were Elav+ neurons (Figure 4C,D). We cannot rule out that *InR* may also be expressed in other cell types, and this profile could also be dynamic.

Using qRT-PCR, we found that *ia-2* RNAi knock-down in neurons did not significantly alter the levels of *dpn* or *elav* mRNA, but decreased the levels of *dilp-6* expression (Figure 4E). The ectopic abdominal Dpn+ cells observed with *ia-2* knock-down (Figure 2H-J) were smaller and had lower Dpn+ levels than normal neural stem cells which were still abundant in the thorax, so any effect in *dpn* mRNA levels in this experiment would have been masked by this background expression, becoming undetectable. Over-expression of *ia-2* in neurons increased the levels of *dpn*, *elav* and *dilp-6* mRNA (Figure 4F). These data were consistent with the in vivo data showing an increase in Dpn+ cells. Importantly, these data showed that *ia-2* function in neurons positively regulates *dilp-6* expression, presumably indirectly. *kon* knock-down in glia reduced *dilp6* mRNA levels even more (Figure 4G),

meaning that *kon* is prominently required for *dilp-6* expression in glia. However, over-expression of full-length *kon* alone was not sufficient to increase the expression of neither *dilp-6* nor *dpn* (Figure 4H), perhaps because the full-length form does not get activated. These data showed that *dilp6* expression depends partly on *ia-2* from neurons, and mostly on *kon* from glia.

Altogether, in the third instar larva Dilp6 is produced by some neurons, but mostly by non-neuropile glia, and it is received at least by InR in neuropile glia. This suggested that an initial ‘Dilp6 signal’ originating from neurons was then amplified by cortex glia and received by neuropile glia. Since both *ia-2* and *Kon* are transmembrane proteins, this raised the question of how this amplification loop may work.

A positive neuron-glia communication loop boosts Dilp-6 production from glia

Signal amplification could occur if Dilp-6 were first secreted from neurons by *ia-2*, to then activate InR in glia, and InR signalling in turn drove the *Kon*-dependent up-regulation of *dilp-6* expression in glia. This would require that *Kon* functions in nuclei to regulate gene expression, but this is not known. Both in mammals and *Drosophila*, NG2 and *Kon* are responsible for glial proliferation (Kucharova and Stallcup, 2010; Losada-Perez, et al., 2016). In mammals, an intracellular domain of NG2 (NG2^{ICD}) is generated upon cleavage of the full-length form (Nayak, et al., 2018; Sakry, et al., 2014). Cytoplasmic NG2^{ICD} interacts with components of the PI3K-Akt-mTOR pathway, to activate protein translation and cell cycle progression (Nayak, et al., 2018; Sakry, et al., 2015). NG2^{ICD} also positively regulates the expression of multiple genes, including downstream targets of mTOR, thus exerting positive feedback (Nayak, et al., 2018; Sakry, et al., 2015), but whether this requires nuclear localization of NG2^{ICD} is unknown. In *Drosophila*, *Kon* had been reported to lack a nuclear localization signal (Schnorrer, et al., 2007). Altogether, whether NG2 or *Kon* regulate glial proliferation and gene expression through cytoplasmic or nuclear events remained unsolved. Thus, to ask whether the intracellular domain of *Kon* (*Kon*^{ICD}) might function in the nucleus, we generated an HA-tagged form of *Kon*^{ICD}. Glial over-expression of *Kon*^{ICD-HA} (*repoGAL4>UAS-Kon*^{ICD-HA}) revealed HA colocalisation with

the glial nuclear transcription factor Repo in neuropile glia cells, showing that Kon^{ICD} was in nuclei (Figure 5A). Next, to test whether Kon^{ICD} is sufficient to induce glial proliferation, we over-expressed it in glia and automatically counted glial cells labeled with the nuclear marker histone-YFP, using DeadEasy software. Over-expression of full-length *kon* induces proliferation and increases glial cell number (Losada-Perez, et al., 2016). Over-expression of *kon*^{ICD} in glia increased glial cell number too (*UAShisYFP; repoGAL4>UASKon*^{ICD}, Figure 5B,C). Thus, Kon^{ICD} can induce glial proliferation. These data showed that Kon can function in the nucleus to regulate *dilp-6* expression, and strongly suggested that full-length Kon is normally cleaved, releasing Kon^{ICD} to promote glial proliferation and regulate gene expression.

Next, to test whether Dilp6 activates InR in glia, we asked: (1) whether over-expression of *dilp-6* could mimic the increase in glial cell number caused by Kon^{ICD}, and (2) whether this could be rescued by over-expression of a dominant negative form of the *insulin receptor* (*InR*^{DN}) in glia. We found that over-expression of *dilp-6* in glial cells increased glial cell number comparably to Kon^{ICD} (Figure 5B,C), and this was rescued with concomitant over-expression of *InR*^{DN} in glia (Figure 5B,C). These data meant that Dilp-6 activates InR signaling in glia, and induces glial proliferation. Dilp6 and InR signaling also reactivate quiescent developmental neural stem cells (Chell and Brand, 2010; Sousa-Nunes, et al., 2011), but Kon functions in glia (Losada-Perez, et al., 2016). To further verify whether Kon function is restricted to glia, we asked whether Kon might also be required in neural stem cells. RNAi *kon* knock-down in neural stem cells with *inscutable-GAL4* (*ins-GAL4>UAS-kon-RNAi*) did not affect the number or distribution of larval Dpn+ cells (Figure 5D,E), meaning that Kon is not required in normal neural stem cells. Since glial proliferation depends on Kon (Losada-Perez, et al., 2016), the fact that *dilp-6* could reproduce the increase in cell number caused by *kon*^{ICD}, and this depended on InR in glia, strongly suggested that InR signalling can activate Kon cleavage downstream, specifically in glia.

To conclude, altogether these data suggested that Ia-2 triggers the release of Dilp-6 from neurons, which then is received by glial cells, where InR signaling activates Kon, which in turn induces

glial proliferation and expression of *dilp-6*. Dilp6 secreted from glia in turn positively feeds-back on glia, further amplifying Dilp-6 production. Thus, a non-autonomous positive feedback loop between neuronal Ia-2 and glial Kon promotes glial proliferation, triggers *dilp-6* expression and sustains Dilp-6 production in glia (Figure 5F). This raised the question of whether neuronal Ia-2 in concert with the Kon-Dilp-6 glial loop only produced more glia, or whether they could also induce neurogenesis.

Ia-2 and Dilp6 can induce neural stem cells from glia

To ask whether Kon, Ia-2 or Dilp6 were responsible for injury-induced non-developmental neurogenesis, we over-expressed them in glia (with *repoGAL4*). Over-expression of full-length *kon* did not induce ectopic Dpn+ cells (Figure 6A-D). By contrast, over-expression of *ia-2* could induce ectopic Dpn+ cells prominently along the midline and in lower levels also in lateral locations surrounding the neuropile, which could be glia (Figure 6A-D). Over-expression of *dilp-6* had an even stronger effect, and there were many Dpn+ cells surrounding the neuropile (Figure 6A-D). Dpn levels in ectopic cells were generally lower than in normal neural stem cells. These data showed that both Ia-2 and Dilp-6 can induce *dpn* expression. However, Kon-full-length alone can't (although this could be due to partial cleavage), meaning that insulin signaling is required to induce neural stem cells. Since Ia-2 drives Dilp-6 production and secretion, this suggested that ultimately Dilp-6 induced neurogenesis.

To further test whether Ia-2 up-regulated *dpn* ectopically via Dilp-6, we carried out epistasis analysis. Over-expression of *ia-2* together with *dilp-6* knock-down in glia (*repoGAL4>UAS-ia-2, UAS-dilp-6-RNAi*), rescued the number of Dpn+ cells (Figure 6A-D), demonstrating that Ia-2 induces neurogenesis via Dilp-6. Furthermore, over-expression of *ia-2* together with *kon* RNAi in glia (*repoGAL4>UAS-ia-2, UAS-konRNAi*) also rescued the Dpn+ phenotype (Figure A-D), consistently with the fact that *dilp-6* expression depends on Kon in glia (see Figure 4G) and that Kon and Dilp6 engage in a positive feedback loop (see Figure 5). Finally, the ectopic Dpn+ phenotype was also rescued by over-expression of *dilp-6* together with *InR^{DN}* in glia (Figure 6A-D, *repoGAL4>UAS-dilp-6, UAS-InR^{DN}*),

meaning that neurogenesis depends on InR signaling in glia. Together, these data showed that *la-2* induces neurogenesis via *Dilp-6* and InR signaling in glia, and that ectopic Dpn originated from glial cells (Figure 5E).

The ectopic Dpn+ cells were distributed along the midline and surrounding the neuropile, in locations that seemed to correspond to glial cells. Thus, to verify this, we tested whether Dpn colocalised with the glial marker Repo. Many of the lateral, ectopic Dpn+ cells observed with *dilp-6* over-expression were also Repo+ (Figure 7A), meaning they originated from glial cells. Dpn levels were lower than in normal neural stem cells. By contrast, the ectopic midline Dpn+ cells were not Repo+ (Figure 7A, magenta cells). This meant that there are two distinct populations of ectopic Dpn+ cells: lateral cells that are neuropile glia, and midline cells which could originate from Repo-negative midline glia.

To further test whether the ectopic neural stem cells originated from glia, we used the cell-lineage marker G-TRACE. This GAL4-dependent tool results in the permanent labeling of UAS-expressing cells and their progeny cells. Thus, *repoGAL4>G-TRACE* marks cells that were once glia, even if the *repo* promoter were to be silenced due to a change to a neuroblast cell state. Cells that were originally glia but may no longer be so would be labelled in green (GFP+), and recently specified glial cells would be labelled in red (RFP+). G-TRACE expression in all neurons with *elavGAL4* or in glia with *repoGAL4* together with *dilp-6* caused larval lethality and thus could not be analysed. By contrast, over-expression of both G-TRACE and *ia-2* in glia (*repoGAL4>G-TRACE, UAS-ia-2*) revealed G-TRACE+ Dpn+ cells around the neuropile (Figure 7C,D). Most of these cells had GFP, but also RFP at somewhat lower levels (Figure 7C,D). These data demonstrate that ectopic Dpn+ were once glial cells. Since RFP was also present, the data also showed that glial cell fate had not been suppressed, and instead suggested that glial cells may be in the process of de-differentiation.

Altogether, these data showed that *la-2*, *Dilp-6*, InR signaling with Kon can induce de novo formation of neural stem cells in neuropile associated glial cells.

DISCUSSION

A critical missing link to understand how to induce CNS regeneration in non-regenerating animals such as humans, had been to identify factors that might interact with NG2 to induce regenerative neurogenesis. NG2 is key because NG2-glia are the only population of progenitor cells that are present throughout life in the adult human brain (Dimou and Gotz, 2014; Torper, et al., 2015; Valny, et al., 2017). Thus, they are the ideal cells to respond to injury and be manipulated to promote regeneration. Still, whether NG2-glia can give rise to neurons is highly debated, and if so, the underlying mechanism was unknown (Dimou and Gotz, 2014; Falk and Gotz, 2017; Valny, et al., 2017; Vigano and Dimou, 2016). Here, using *Drosophila* in vivo functional genetic analysis we have identified neuronal *la-2* and insulin signaling as the key interactors of the NG2 homologue *kon*, that can induce neurogenesis from NG2-like glial cells.

We provide evidence that *la-2* is a neuronal partner of *Kon* responsible for inducing neurogenesis from NG2-like glia after CNS injury (Figure 8A). We show that in the un-injured CNS, *Kon* and *la-2* mutually repress each other's expression, confining each other to glia and neurons, respectively. Normal levels of *ia-2* are required to prevent the non-autonomous induction of neural stem cells from neighbouring glial cells. A reduction in *ia-2* levels non-autonomously increases *kon* expression, which up-regulates *dilp-6* from glia; an increase in *ia-2* levels up-regulates Dilp-6 secretion and production from neurons. Either way, the consequence is raised Dilp-6, which switches on a positive amplification loop from glia that results in further Dilp-6 production. Thereafter, Dilp6 can induce *dpn* expression in glia. Injury causes an up-regulation in *ia-2* expression, as well as *kon* (Losada-Perez, et al., 2016)(Figure 8B). *la-2* drives secretion of Dilp-6 from neurons, and an amplification positive feedback loop involving *Kon*, Dilp6 and InR drives the further *Kon*-dependent production of Dilp-6 from cortex glia. Dilp-6 increases *Kon*-dependent glial proliferation, meaning that InR signaling may facilitate *Kon* cleavage. Dilp-6 also triggers InR signaling and the expression of the neural stem cell marker *dpn* in neuropile – but not cortex - glia (Figure 8B,C). *Dpn* is a bHLH transcriptional repressor of neuronal differentiation, and common neural stem marker in *Drosophila*

(Sousa-Nunes, et al., 2010). Ectopic Dpn+ cells are found upon injury and genetic manipulation of *la-2* and *Dilp-6*. We show that these ectopic Dpn+ cells originate from glia. Altogether, this relay from neurons to cortex and then to neuropile glia enables concerted glio- and neuro-genesis, matching interacting cell populations for regeneration (Figure 8B).

In vertebrates and also in invertebrates, neural stem cells found after development in the adult CNS and upon injury, are generally distinct from developmental ones, and can originate from hemocytes, but most often, from glial cells (Falk and Gotz, 2017; Simoes and Rhiner, 2017; Tanaka and Ferretti, 2009). Our findings that *Dilp6* and *InR* can induce *dpn* expression are reminiscent of their functions in the induction of neural stem cells from quiescent progenitors in development (Chell and Brand, 2010; Gil-Ranedo, et al., 2019; Sousa-Nunes, et al., 2011). However, the Dpn+ cells induced upon injury and after development, are distinct from the developmental neural stem cells normally induced by *Dilp-6*. Firstly, in injuries carried out in third instar larvae, the induced neural stem cells were more numerous than normal neural stem cells. Secondly, in injuries carried out late in wandering larvae, Dpn+ cells were found after normal developmental neural stem cells have been eliminated through apoptosis (Bello, et al., 2003). Thirdly, in both cases Dpn+ cells were found in ectopic locations not normally occupied by developmental neural stem cells (Bello, et al., 2003). For instance, ectopic Dpn+ cells often occupied dorsal positions over the neuropile. Ectopic Dpn+ cells were located along the midline and surrounding the neuropile, in positions that correspond to, possibly midline, and often neuropile glia. Indeed, our data demonstrated that at least the non-midline ectopic Dpn+ originate from glial cells: 1, all ectopic Dpn+ cells from genetic manipulations did not have *la-2-YFP*, which is expressed in all neurons. The fact that upon injury, a minority of ectopic Dpn+ cells were also *la-2YFP+* could mean that upon injury *la-2* is over-expressed also in glia, or that as neurons acquire Dpn they down-regulate *la-2*. 2, Ectopic Dpn+ cells surrounded the neuropile, occupying positions of neuropile glia; 3, Repo-negative Dpn+ cells occupied positions along the midline, characteristic of midline glia; 4, all Dpn+ cells surrounding the neuropile also had

Repo; 5, lineage tracing with G-TRACE demonstrated that ectopic Dpn+ cells originated from glial cells.

In principle, regenerative neurogenesis could occur via direct conversion of glia into neurons, glial de-differentiation, or neuronal de-differentiation. Neuronal de-differentiation occurs both in mammals and in *Drosophila* (Froldi, et al., 2015). However, in mammals, neurogenesis after development and in response to injury most often originates from glial cells (Dimou and Gotz, 2014; Falk and Gotz, 2017; Tanaka and Ferretti, 2009). In the adult mammalian brain, radial glia in the hippocampus respond to environmental challenge by dividing asymmetrically to produce neural progenitors, that produce neurons (Shtaya, et al., 2018). Astrocytes and NG2 glia can generate neurons in response to stroke or excitotoxic injury, and genetic manipulations (Dimou and Gallo, 2015; Heinrich, et al., 2014; Peron and Berninger, 2015). Genetic manipulation can lead to the direct conversion of NG2 glia into neurons that integrate into functional neural circuits (Pereira, et al., 2017; Torper, et al., 2015). Importantly, injury creates a distinct cellular environment that prompts glial cells to generate different cell types than in the un-injured CNS. For instance, elevated Sox-2 is sufficient to directly reprogramme NG2 glia into neurons, but only upon injury (Heinrich, et al., 2014). And whereas during normal development NG2 glial cells may only produce oligodendrocyte lineage cells, upon injury they can produce also astrocytes and neurons (Dimou and Gallo, 2015; Huang, et al., 2018). What the injury cues are, is unknown.

In our context in the *Drosophila* larva, Dpn may not be sufficient to carry neurogenesis through. Firstly, loss of *ia-2* function resulted in ectopic Dpn+ and Pros+ cells that could be ganglion mother cells as well as neural stem cells, but gain of *ia-2* function resulted only in Dpn+ cells but not Pros+. This suggested that *ia-2* and Dpn are not sufficient for neuroblasts to progress to ganglion mother cells. Secondly, alterations in *ia-2* levels induced ectopic Dpn+ cells, but not ectopic Eve+ neurons. And finally, ectopic Dpn+ cells still had also Repo. These data suggest that to generate neurons, glia not only require to express *dpn*, but also to receive other yet unknown signals for neuronal differentiation (Figure 8B). A limitation of injury in the larval VNC is time. Injury is best

carried out in the late larva to avoid interference with developmental neuroblasts. However, just a few hours after injury, larvae pupate. Cells may not have enough time to go through neuronal lineages from neural stem cell to differentiated neuron. Pupariation and metamorphosis bring in a different cellular context that could interfere with regeneration. With our data, we can conclude that a neuron-glia communication loop involving *la-2*, *Dilp-6*, *Kon* and *InR* is responsible for the induction of the neural stem cell marker *Dpn* in glia.

Our work has revealed a key link between Notch, Pros, Kon and insulin signaling to drive regenerative neurogenesis from glia. *la-2* has universal functions in dense core vesicles to release insulin and neurotransmitters (Cai, et al., 2011; Cai, et al., 2001; Harashima, et al., 2005; Kim, et al., 2008; Nishimura, et al., 2010). *Dilp-6* reactivates quiescent developmental neural stem cells in *Drosophila* (Chell and Brand, 2010; Sousa-Nunes, et al., 2011), and in mammals, insulin-like growth factor 1 (IGF-1) induces the production of astrocytes, oligodendrocytes and neurons from progenitor cells in the adult brain, also in response to exercise (Mir, et al., 2017; Nieto-Estevez, et al., 2016). The transcription factor Sox-2 that can switch astrocytes to becoming neural stem cells and produce neurons, is a downstream effector of *InR*/AKT signaling (Mir, et al., 2017). Together, these findings mean that insulin signaling is involved in switching glial cells into becoming neural stem cells. Intriguingly, *dpn* was induced only in neuropile associated glial cells, but not in cortex glia. Neuropile glia proliferate upon injury, to regenerate glial cells (Kato, et al., 2011; Losada-Perez, et al., 2016). Thus, some Repo+ glia cells may produce only glia after injury, and those that become *Dpn*+ cells could give rise to both neurons and glia. Neuropile glia, identified by the *alrmGAL4* driver and known as *Drosophila* astrocytes, uniquely express Notch, Pros and Kon, as well as *InR*, and we showed that *la-2* is functionally linked to these genes. In mammals, the combination of Notch1, Prox1 and NG2 is unique to NG2-glia, also after development, and is absent from astrocytes (Cahoy, et al., 2008). This would suggest that *la-2* and *Dilp-6* can only induce *dpn* in NG2-like glia bearing this combination of factors. In fact, *dpn* is regulated by both Notch and Pros: Notch activates *dpn* expression promoting stemness, and Pros inhibits it, promoting transition to ganglion mother cell and neuron (Babaoglan,

et al., 2013;Bi and Kuang, 2015;San-Juan and Baonza, 2011;Vaessin, et al., 1991). Thus, only glial cells with Notch and Pros may be poised to modulate stemness and neuronal differentiation.

Notch, Kon and Pros regulate glial proliferation in response to injury (Kato, et al., 2011;Losada-Perez, et al., 2016), and *la-2* is functionally related to them (Figure 1). In the mammalian CNS, Notch determines NG2-glia proliferation and maintains the progenitor state, whereas its downregulation is required to induce both glial and neuronal differentiation following proliferation (Ables, et al., 2010;Falk and Gotz, 2017;Piccin, et al., 2013;Yamamoto, et al., 2001). Notch also activates *kon* expression (Losada-Perez, et al., 2016). NG2 interacts with AKT and other downstream components of the InR signalling pathway to promote protein synthesis and cell cycle progression, and to regulate the expression of its downstream effectors in a positive feedback loop (Nayak, et al., 2018). Insulin signaling also activates *dpn* expression, by repressing FoxO, which represses *dpn* (Siegrist, et al., 2010). Consistent with these data, we have shown that in glia, the ability of Dilp-6 and InR to induce glial proliferation depends on Kon, and that Kon drives positive feedback on insulin signaling by regulating *dilp-6* expression. Importantly, Kon does not appear to function in developmental neural stem cells. As Notch, Pros and insulin signaling are known to positively regulate *dpn* expression (Siegrist, et al., 2010; Babaoglan, et al., 2013;Bi and Kuang, 2015;San-Juan and Baonza, 2011;Vaessin, et al., 1991), and injury induces a Notch-dependent up-regulation of Kon (Losada-Perez, et al., 2016), our data suggest that the Notch-Kon-InR synergy can trigger the activation of *dpn* expression. Induced neural stem cells thereafter would have the potential to generate only glia from daughter cells that have Kon and Pros, on which Repo and glial cell fate depend, or neurons, from daughter cells that lack Kon, and express Pros on which *la-2* depends (Figure 8B). Thus, upon injury, *la-2*, insulin signalling, Notch, Pros and Kon functioning together enable the regenerative production of both more glial cells, and of neural stem cells from glia (Figure 8B,C).

To conclude, we have shown that *la-2* triggers two distinct responses in glia: in glial cells with Kon, *la-2* and insulin signaling boost Kon-dependent glial proliferation and amplification of Dilp-

6. In NG2-like glial cells that also express Notch and Pros, their combination with Kon and insulin signaling in response to Ia-2 also unlocks their neurogenic potential, inducing neural stem cell fate. As a result, these genes could drive the production of both glial cells and neurons after injury, enabling the matching of interacting cell populations, which is essential for regeneration.

MATERIALS AND METHODS

Fly stocks and genetics. Fly stocks used are listed in Table 1 below. Stocks carrying combinations of over-expression and RNAi, or RNAi and mutants, etc., were generated by conventional genetics. N^{ts} mutants were raised at 18°C to enable normal embryogenesis, and switched to 25°C from larval hatching to the third instar larval wandering stage to cause N loss of function. For all experiments, larvae bearing balancer chromosomes were identified by either using the fluorescent balancers CyO Dfd-YFP and TM6B Dfd-YFP or using the balancer SM6a-TM6B Tb⁻, which balances both the second and third chromosomes, and discarded. For the genetic screens, larvae with fluorescent VNCs (i.e. repoGAL4>UAS-FlyBow or elavGAL4>UAS-FlyBow) were selected.

What	Genotype	From
Control	yw	Hidalgo lab
Mutants	kon ^{c452} /CyO, Dfd-YFP	Losada-Perez et al 2016
	ia-2 deficiency: w ¹¹¹⁸ ; P{w ^{+mW.Scer\FRT.hs3} =3'.RS5+3.3'}ED7733 / SM6a	Kyoto DGRC 150199
	pros ^{S044116} /TM6B	Kato et al, 2011
	pros ^{voila1} /TM6B	Kato et al, 2011
Reporter	Notch ^{ts1} /FM7(sn ⁺) actGFP	Kato et al, 2011
GAL4 drivers	IA2-YFP: w ¹¹¹⁸ ; PBac{566.P.SVS-1}ia-2CPTI100013	Kyoto DGRC 115077
	Neurons: w;;elavGal4	Hidalgo lab
	Glia: w;;repoGal4/TM6B	Hidalgo lab
	w Dilp-6Gal4/FM7	Kyoto DGRC 103877
	w*; P{GawB}InRNP2552 / TM6B	Kyoto DGRC 104236
UAS lines	w*; P{GawB}insc [Mz1407]	BSC 8751
	UAS-ia-2: w;; UASia-2-@attp2/SM6aTM6B	This work
	UAS-ia-2: y ¹ w ^{67c23} ; P{GSV6}GS11438/SM1	Kyoto DGRC 203335
	w; UASpros-k	Kato et al, 2011
	w; UAS-HA-Kon FL4-1/TM3 Twi-GFP	Losada-Perez et al 2016
	w; UAShistone-YFP	Kato et al, 2011
	w; UAS kon-ICD::HA	This work
	y ¹ w ¹¹¹⁸ ; UAS-dilp-6	Gift of Alex Gould
	y ¹ w ¹¹¹⁸ ; P{UAS-InR.K1409A}2	BSC 8252
G-TRACE: w[*]; P{w[+mC]=UAS-RedStinger}4, P{w[+mC]=UAS-FLP.D}JD1, P{w[+mC]=Ubi-p63E(FRT.STOP)Stinger}9F6/CyO	BSC 28280	

UAS-RNAi lines	UAS-ia-2-RNAi: $y^1sc^1v^1$; P{TRIP HM50V536} attP2	BSC 33672
	UAS-konRNAi:P{KK102101}VIE-260B	VDRC
	UAS-Dilp6-RNAi: P{KK111727}VIE-260B	VDRC
	UAS-ptp4E RNAi: yscv;;P{TripHMSO1838}attp2	BSC 38369
	UAS-ptp10D RNAi: yscv;;P{TripHMSO1917}attp2	BSC 39001
	UAS-ptp61F RNAi: yscv;;P{TripHMCO43446}attp2	BSC
	UAS-ptp69A RNAi: yv;;P{TripJFO3399}attp2	BSC 29462
	UAS-ptp99A RNA: yv;;p{Trip1858}attp2	BSC 25840
	UAS-Hpo RNAi: yv;;p{TripHMSO0006}attp2	BSC 33614
	UAS-Prl-1 RNAi: yscvp;;{TripPMAS01826}attp2/TM3,Sb	BSC 38358
	UAS-Lar RNAi: w/yv;;p{TripHMSO2156}attp2	BSC 40938
	UAS- PP2A-B' RNAi: yw;;p{TripHMO5256}attp2	BSC
	UAS- GRIP RNAi:yw;;P{tRiPjfo2969}attp2	BSC 28334
	UAS-Akap200 RNAi: yv;;p{TripHMSO18}attp2	BSC 28532
	UAS-arfrp1 RNAi: y[1] v[1]; P{y[+t.7] v[+t.1.8]=TRiP.JF02651}attP2	BSC 27501
	UAS-cadN RNAi: y v[+t.1.8]=TRiP.JF02653}attP2	BSC 27503
	UAS-cadN2 RNAi: y v[+t.1.8]=TRiP.JF02658}attP2	BSC 27508
	UAS-cerk RNAi: y v[+t.1.8]=TRiP.GL00273}attP2	BSC 35361
	UAS-CG42327 RNAi: y v[+t.1.8]=TRiP.HMS00227}attP2	BSC 33356
	UAS-ds RNAi: y v[+t.1.8]=TRiP.HMS00759}attP2	BSC 32964
	UAS-eya RNAi: y v[+t.1.8]=TRiP.JF03160}attP2	BSC 28733
	UAS-eyes RNAi: y v[+t.1.8]=TRiP.JF01069}attP2	BSC 31513
	UAS-fak56D RNAi: y v[+t.1.8]=TRiP.JF02484}attP2	BSC 29323
	UAS-ft RNAi: y v[+t.1.8]=TRiP.JF03245}attP2	BSC 29566
	UAS-fu12 RNAi : y v[+t.1.8]=TRiP.HMC04917}attP40	BSC 57728
	UAS-fz RNAi: y v[+t.1.8]=TRiP.HMS01308}attP2	BSC 34321
	UAS-if RNAi: y v[+t.1.8]=TRiP.JF02695}attP2	BSC 27544
	UAS-inaD RNAi: y v[+t.1.8]=TRiP.HMC03170}attP2	BSC 52313
	UAS-kul RNAi: y v[+t.1.8]=TRiP.HMC03803}attP40	BSC 55653
	UAS-kuz RNAi: w; P{KK103555}VIE-260B	VDRC
	UAS-metro RNAi: y v[+t.1.8]=TRiP.HMC04629}attP40	BSC 57242
	UAS-mew RNAi: y v[+t.1.8]=TRiP.JF02694}attP2	BSC 27543
	UAS-mtm RNAi: y v[+t.1.8]=TRiP.JF01114}attP2	BSC 31552
	UAS-mys RNAi: y v[+t.1.8]=TRiP.JF02819}attP2	BSC 27735
	UAS-sdc RNAi: y v[+t.1.8]=TRiP.HMC03265}attP2	BSC 51723
	UAS-wnt5 RNAi: y v[+t.1.8]=TRiP.HMS01119}attP2	BSC 34644
	UAS-wde RNAi: y v[+t.1.8]=TRiP.HMS00205}attP2	BSC 33339
	UAS-vang RNAi: y v[+t.1.8]=TRiP.HMS01343}attP2	BSC 34354
	UAS-stan RNAi: y v[+t.1.8]=TRiP.JF02047}attP2	BSC 26022
	UAS-ssu72 RNAi: y v[+t.1.8]=TRiP.HMS04461}attP40	BSC 57018
	UAS-shg RNAi: y v;;TRiP.JF02769}attP2/TM3, Sb[1]	BSC 27689
	UAS-psn RNAi: y v;; TRiP.JF02760}attP2/TM3, Sb[1]	BSC 27681
	UAS-prosbeta7 RNAi: y v[+t.1.8];;TRiP.HMS00122}attP2	BSC 34812
	UAS-prl-1 RNAi: y v TRiP.HMS01826}attP2/TM3, Sb[1]	BSC 38358
	UAS-lar RNAi : y v[+t.1.8]=TRiP.HMS02186}attP40	BSC 40938
	UAS-lanB2 RNAi: y v[+t.1.8]=TRiP.HMC04076}attP40	BSC 55388
	UAS-lanA RNAi: y v[+t.1.8]=TRiP.JF02908}attP2	BSC 28071

Crush injury in the larval VNC. Crush injury in the larval CNS was carried out as previously reported (Losada-Perez, et al., 2016), and only lesions in the abdominal VNC were analysed. Larval collections were staged by putting the Go flies in an egg laying chamber for 2h, then collecting the F1 larvae 74h

later. Crush injury was carried out: (1) at 74-76h after egg laying (AEL); after injury, VNCs were left to carry on developing at 25°C, and were dissected 5-7h later; (2) at 96 h, and after injury they were incubated at 25°C and dissected and fixed 6h later; (3) at 117h AEL, and after injury, were incubated at 25°C, and dissected 12 hours later. Dissected and fixed VNC when then processed for antibody stainings following standard procedures.

Molecular cloning

The UAS-konICD-Venus constructs were generated from EST LD31354 via PCR amplification with Kappa HiFi PCR kit (Peqlab) and subsequent cloning using the Gateway cloning system (Invitrogen) according to manufacturers instructions. Primers used were kon^{ICD} fwd comprising the CACC-sequence at the 5'-end (CCACAGGAACTGAGAAAGCACAAGGC) for direct cloning of the PCR product (482 bp) into the entry vector pENTR/D-Topo, and kon^{ICD} rev (AAACCTTACACCCAATACTGATTCC) including the endogenous stop-codon, underlined. Destination vector was pTVW for tagging the ICD on the N-terminus with Venus, including a 5xUAS cassette and P-element ends for transformation. These destination vectors were developed by the Murphy-Lab at Carnegie Institution of Science, Baltimore, MD, USA, and can be obtained from Drosophila Genomics Resource Center at Indiana University, USA. Transformant fly strains were generated by BestGene Inc, Chino Hills, CA, USA following a standard transposase-mediated germline transformation protocol.

A UAS-ia-2 construct was generated using Gateway cloning (Invitrogen, as above). ia-2 cDNA was generated by reverse-transcription PCR from purified mRNA from Oregon R flies, and cloned into pDONR. Subsequently, a standard PCR amplification was performed using Phusion High-Fidelity (Fisher Scientific), primers ia-2F (5'- ATGGCACGCAATGTACAACAACGGC) and ia-2-stopR (5' - CTTCTTCGCCTGCTTCGCCGATTG), and the resulting PCR product (3918bp) was cloned into pGEM[®]-T Easy Vector (Promega). Subsequently, a Phusion High Fidelity PCR amplification was carried out using Gateway primers ia-2attB F1 (5' - ggggacaagttgtacaaaaagcaggcttcATGGCACGCAATGTACAACAACGGC) and ia-2attB R1 (5' -

ggggaccactttgtacaagaaagctgggtcCTTCTTCGCTGCTTCGCCGATTG), and plasmid pGEM-ia-2 as template. Using Gateway cloning, the PCR product (3979bp) was cloned into first pDONR²²¹ and subsequently into the pUAS-gw-attB destination vector, for ϕ C31 transgenesis. The construct was injected by BestGene, to generate transgenic flies bearing UAS-ia-2 at the attP2 landing site.

Quantitative real time reverse transcription PCR (qRT-PCR).

qRT-PCR was performed according to standard methods and as previously described (Losada-Perez, et al., 2016), with the following alteration. For each sample, 10 third instar larvae were used per genotype per replicate. At least three independent biological replicates were performed for all experiments other than in Supplementary Figure S3A and B where two replicates were carried out on all candidates and those of interest were taken forward to carry out two further replicates. For a list of the primers used in this study please see Table 2 below:

Table 2 Primers	
PRIMER	SEQUENCE 5' TO 3'
RpL32qPCRf	AAGCGGCGACGCACTCTGTT
RpL32qPCRR	AAGCGGCGACGCACTCTGTT
GAPDH2F qPCR	GCCCAGCATACAGGCCCAAG
GAPDH2R qPCR	GTGAAGCTGATCTCTTGGTACGAC
KonqPCR(Ex10-11) F3	CCGCGCCCTAATCTTTAACTTTTAC
KonqPCR(Ex10-11) F3	CCCAAGCGATTTCTTTACCA
ptp99A qPCR F2	TCGCTATCCCAACATCACGG
ptp99A qPCR R2	TGAACGCATGTCCCTTCTGG
Fz qPCR F1	AGTCGCACTTATTCCACCTGG
Fz qPCR R1	CTGGCCCACGAAACAAACG
Hippo qPCR F2	ACCCATAGCCACAGAGTATTCT
Hippo qPCR R2	TGCTGTTTCATCCTGCTGTTG
ia-2 qPCR F1	ACGGTCACCCAGTTTCACTT
ia-2 qPCR R1	CGGTAGGACTTGTTCACTTTCC
InaD qPCR F1	TCATTGAGTTGAAGGTGGAAAAGA
InaD qPCR R1	CTGCCACTTGTCCCTCCG
Iar qPCR F1	TTGCTGAGTACAACATGCCG
Iar qPCR R1	TGAAGTCGATGAAGCCCTCG
Prl-1 qPCR F1	TGACGAGTGGTTTGAGGTCTTAA
Prl-1 qPCR R1	GCCCAATTCAATCAGTGCCA
Ptp10D qPCR F1	TGCAACAGATCAACACGTCTG
Ptp10D qPCR R1	TATACTGCTGCTCCGTCTGC
Ptp61F qPCR F1	GTCCAAGGTGCTCTGCGAG
Ptp61F qPCR R1	ATGAGGGGTTCTTCAGCGTC

Ptp69D qPCR F1	TGTAGTGTGGGCGAAAACGA
Ptp69D qPCR R1	CGCATCGGAAGTGGTGTAG
Yorkie qPCR F1	ATCAGCCCCATTTCAGTTGAAC
Yorkie qPCR R1	CCTCCCACTGCGTAGATTTTGTA
Dpn qPCR F1	ACGCATGTCCAATCCCAATG
Dpn qPCR R2	GCGACGTTTCTCCATAATCGGT
Elav qPCR F1	CTACTTGCCGCAAACAATGAC
Elav qPCR R1	CTTCACCGACTCAATCTCGC
dilp6 qPCR F1	CGATGTATTTCCCAACAGTTTCG
dilp6 qPCR R1	AAATCGGTTACGTTCTGCAAGTC

Immunostainings were carried out following standard procedures. The following primary antibodies were used: mouse anti-Repo (1:100, DSHB); guinea pig anti-Repo (1:1000, Ben Altenhein); rat anti-Elav (1:250, DSHB); mouse anti-FasII ID4 (1:500, DSHB); mouse anti-Prospero (1:250, DSHB); guinea pig anti-Dpn (1:1000, gift of J. Skeath); mouse anti-Eve 3C10 (1:20, DSHB); rabbit anti-GFP at 1:250 (Molecular Probes). Secondary antibodies were Alexa conjugated: Donkey anti-rabbit 488 (1:250, Molecular Probes), goat anti-mouse 488 (1:250, Molecular Probes), goat anti-mouse 647 (1:250, Molecular Probes), goat anti-guinea pig 488 (1:250, Molecular Probes), goat anti-guinea pig 633 (1:250, Molecular Probes), goat anti-rat 647 (1:250, Molecular Probes).

Microscopy and imaging. Image data were acquired using Zeiss LSM710 and Leica SP8 laser scanning confocal microscopes, using a 25x lens, 1.25 zoom, resolution 512x512 or 1024x1024, step 0.96 μ m and 3x averaging for all samples except for cell counting with DeadEasy that have no averaging.

Images were analysed using ImageJ. Images of horizontal sections are projections from the stacks of confocal images that span the thickness of the entire VNC, using ImageJ. Transverse views were generated using the Reslice option. Images were processed using Adobe Creative Suite 6 Photoshop and compiled with Adobe Illustrator.

Automatic cell counting

Glial cells labelled either with anti-Repo or with repoGAL4>UAShistone-YFP were counted automatically in 3D across the thickness of the VNC using DeadEasy Larval Glia software, as

previously described. Prospero+ and Dpn+ cells were counted manually in 3D (i.e. not in projections), as the signal was noisy for DeadEasy.

Statistical analysis

Statistical analysis was carried out using Graphpad Prism. All data in this work are continuous. Tests to determine whether data were distributed normally and variances were equal were initially carried out, and thereafter if so, parametric One Way ANOVA tests were carried when comparing more than two sample types group. Multiple comparison corrections were carried out with post-hoc Dunnett tests comparisons to set controls, or Bonferroni comparisons of all samples against all. Box plots were used to represent the distribution of data.

ACKNOWLEDGEMENTS

We thank our labs and C. Rezaval for discussions and comments on the manuscript; S. Corneliusen, T. Schunke and S. Dietz and for technical help; Y. Jan, J. Skeath, A. Gould and F. Schnorrer for reagents; Bloomington Drosophila Stock Centre for fruit-flies and Developmental Studies Hybridoma Bank, Iowa for antibodies.

FUNDING

This work was funded by BBSRC Project Grants BB/L008343/1 and BB/R00871X/1 to A.H., and BBSRC MIBTP PhD studentship to E.C.

REFERENCES

Ables, JL, Decarolis, NA, Johnson, MA, Rivera, PD, Gao, Z, Cooper, DC, Radtke, F, Hsieh, J and Eisch, AJ.(2010). Notch1 is required for maintenance of the reservoir of adult hippocampal stem cells. *J Neurosci* **30**, 10484-10492 [10.1523/JNEUROSCI.4721-09.2010](https://doi.org/10.1523/JNEUROSCI.4721-09.2010)

Babaoglan, AB, Housden, BE, Furriols, M and Bray, SJ.(2013). Deadpan contributes to the robustness of the notch response. *PLoS One* **8**, e75632 [10.1371/journal.pone.0075632](https://doi.org/10.1371/journal.pone.0075632)

- Bello, BC, Hirth, F and Gould, AP.(2003). A pulse of the Drosophila Hox protein Abdominal-A schedules the end of neural proliferation via neuroblast apoptosis. *Neuron* **37**, 209-219
- Bi, P and Kuang, S.(2015). Notch signaling as a novel regulator of metabolism. *Trends Endocrinol Metab* **26**, 248-255 10.1016/j.tem.2015.02.006
- Biname, F, Sakry, D, Dimou, L, Jolivel, V and Trotter, J.(2013). NG2 regulates directional migration of oligodendrocyte precursor cells via Rho GTPases and polarity complex proteins. *J Neurosci* **33**, 10858-10874 10.1523/JNEUROSCI.5010-12.2013
- Boone, JQ and Doe, CQ.(2008). Identification of Drosophila type II neuroblast lineages containing transit amplifying ganglion mother cells. *Dev Neurobiol* **68**, 1185-1195 10.1002/dneu.20648
- Cahoy, JD, Emery, B, Kaushal, A, Foo, LC, Zamanian, JL, Christopherson, KS, Xing, Y, Lubischer, JL, Krieg, PA, Krupenko, SA, Thompson, WJ and Barres, BA.(2008). A transcriptome database for astrocytes, neurons, and oligodendrocytes: a new resource for understanding brain development and function. *J Neurosci* **28**, 264-278 10.1523/JNEUROSCI.4178-07.2008
- Cai, T, Hirai, H, Fukushige, T, Yu, P, Zhang, G, Notkins, AL and Krause, M.(2009). Loss of the transcriptional repressor PAG-3/Gfi-1 results in enhanced neurosecretion that is dependent on the dense-core vesicle membrane protein IDA-1/IA-2. *PLoS Genet* **5**, e1000447 10.1371/journal.pgen.1000447
- Cai, T, Hirai, H, Zhang, G, Zhang, M, Takahashi, N, Kasai, H, Satin, LS, Leapman, RD and Notkins, AL.(2011). Deletion of Ia-2 and/or Ia-2beta in mice decreases insulin secretion by reducing the number of dense core vesicles. *Diabetologia* **54**, 2347-2357 10.1007/s00125-011-2221-6
- Cai, T, Krause, MW, Odenwald, WF, Toyama, R and Notkins, AL.(2001). The IA-2 gene family: homologs in Caenorhabditis elegans, Drosophila and zebrafish. *Diabetologia* **44**, 81-88 10.1007/s001250051583
- Carmona, GN, Nishimura, T, Schindler, CW, Panlilio, LV and Notkins, AL.(2014). The dense core vesicle protein IA-2, but not IA-2beta, is required for active avoidance learning. *Neuroscience* **269**, 35-42 10.1016/j.neuroscience.2014.03.023
- Chell, JM and Brand, AH.(2010). Nutrition-responsive glia control exit of neural stem cells from quiescence. *Cell* **143**, 1161-1173 10.1016/j.cell.2010.12.007
- Dimou, L and Gallo, V.(2015). NG2-glia and their functions in the central nervous system. *Glia* **63**, 1429-1451 10.1002/glia.22859
- Dimou, L and Gotz, M.(2014). Glial cells as progenitors and stem cells: new roles in the healthy and diseased brain. *Physiol Rev* **94**, 709-737 10.1152/physrev.00036.2013
- Falk, S and Gotz, M.(2017). Glial control of neurogenesis. *Curr Opin Neurobiol* **47**, 188-195 10.1016/j.conb.2017.10.025
- Froldi, F, Szuperak, M, Weng, CF, Shi, W, Papenfuss, AT and Cheng, LY.(2015). The transcription factor Nerfin-1 prevents reversion of neurons into neural stem cells. *Genes Dev* **29**, 129-143 10.1101/gad.250282.114

- Gage, FH.(2019). Adult neurogenesis in mammals. *Science* **364**, 827-828 10.1126/science.aav6885
- Gil-Ranedo, J, Gonzaga, E, Jaworek, KJ, Berger, C, Bossing, T and Barros, CS.(2019). STRIPAK Members Orchestrate Hippo and Insulin Receptor Signaling to Promote Neural Stem Cell Reactivation. *Cell Rep* **27**, 2921-2933 e2925 10.1016/j.celrep.2019.05.023
- Griffiths, RL and Hidalgo, A.(2004). Prospero maintains the mitotic potential of glial precursors enabling them to respond to neurons. *EMBO J* **23**, 2440-2450 10.1038/sj.emboj.7600258
- Harashima, S, Clark, A, Christie, MR and Notkins, AL.(2005). The dense core transmembrane vesicle protein IA-2 is a regulator of vesicle number and insulin secretion. *Proc Natl Acad Sci U S A* **102**, 8704-8709 10.1073/pnas.0408887102
- Heinrich, C, Bergami, M, Gascon, S, Lepier, A, Vigano, F, Dimou, L, Sutor, B, Berninger, B and Gotz, M.(2014). Sox2-mediated conversion of NG2 glia into induced neurons in the injured adult cerebral cortex. *Stem Cell Reports* **3**, 1000-1014 10.1016/j.stemcr.2014.10.007
- Henquin, JC, Nenquin, M, Szollosi, A, Kubosaki, A and Notkins, AL.(2008). Insulin secretion in islets from mice with a double knockout for the dense core vesicle proteins islet antigen-2 (IA-2) and IA-2beta. *J Endocrinol* **196**, 573-581 10.1677/JOE-07-0496
- Hidalgo, A and Logan, A.(2017). Go and stop signals for glial regeneration. *Curr Opin Neurobiol* **47**, 182-187 10.1016/j.conb.2017.10.011
- Hu, YF, Zhang, HL, Cai, T, Harashima, S and Notkins, AL.(2005). The IA-2 interactome. *Diabetologia* **48**, 2576-2581 10.1007/s00125-005-0037-y
- Huang, W, Bai, X, Stopper, L, Catalin, B, Cartarozzi, LP, Scheller, A and Kirchhoff, F.(2018). During Development NG2 Glial Cells of the Spinal Cord are Restricted to the Oligodendrocyte Lineage, but Generate Astrocytes upon Acute Injury. *Neuroscience* **385**, 154-165 10.1016/j.neuroscience.2018.06.015
- Kato, K, Forero, MG, Fenton, JC and Hidalgo, A.(2011). The glial regenerative response to central nervous system injury is enabled by pros-notch and pros-NFkappaB feedback. *PLoS Biol* **9**, e1001133 10.1371/journal.pbio.1001133
- Kato, K, Konno, D, Berry, M, Matsuzaki, F, Logan, A and Hidalgo, A.(2015). Prox1 Inhibits Proliferation and Is Required for Differentiation of the Oligodendrocyte Cell Lineage in the Mouse. *PLoS One* **10**, e0145334 10.1371/journal.pone.0145334
- Kato, K, Losada-Perez, M and Hidalgo, A.(2018). Gene network underlying the glial regenerative response to central nervous system injury. *Dev Dyn* **247**, 85-93 10.1002/dvdy.24565
- Kim, J, Bang, H, Ko, S, Jung, I, Hong, H and Kim-Ha, J.(2008). Drosophila ia2 modulates secretion of insulin-like peptide. *Comp Biochem Physiol A Mol Integr Physiol* **151**, 180-184 10.1016/j.cbpa.2008.06.020
- Kucharova, K, Chang, Y, Boor, A, Yong, VW and Stallcup, WB.(2011). Reduced inflammation accompanies diminished myelin damage and repair in the NG2 null mouse spinal cord. *J Neuroinflammation* **8**, 158 1742-2094-8-158 [pii] 10.1186/1742-2094-8-158

Kucharova, K and Stallcup, WB.(2010). The NG2 proteoglycan promotes oligodendrocyte progenitor proliferation and developmental myelination. *Neuroscience* **166**, 185-194
10.1016/j.neuroscience.2009.12.014

Losada-Perez, M, Harrison, N and Hidalgo, A.(2016). Molecular mechanism of central nervous system repair by the Drosophila NG2 homologue kon-tiki. *J Cell Biol* **214**, 587-601 10.1083/jcb.201603054

Mir, S, Cai, W, Carlson, SW, Saatman, KE and Andres, DA.(2017). IGF-1 mediated Neurogenesis Involves a Novel RIT1/Akt/Sox2 Cascade. *Sci Rep* **7**, 3283 10.1038/s41598-017-03641-9

Mooney, RA, Kulas, DT, Bleye, LA and Novak, JS.(1997). The protein tyrosine phosphatase LAR has a major impact on insulin receptor dephosphorylation. *Biochem Biophys Res Commun* **235**, 709-712
10.1006/bbrc.1997.6889

Nayak, T, Trotter, J and Sakry, D.(2018). The Intracellular Cleavage Product of the NG2 Proteoglycan Modulates Translation and Cell-Cycle Kinetics via Effects on mTORC1/FMRP Signaling. *Front Cell Neurosci* **12**, 231 10.3389/fncel.2018.00231

Nieto-Estevez, V, Defterali, C and Vicario-Abejon, C.(2016). IGF-I: A Key Growth Factor that Regulates Neurogenesis and Synaptogenesis from Embryonic to Adult Stages of the Brain. *Front Neurosci* **10**, 52 10.3389/fnins.2016.00052

Nishimura, T, Harashima, S, Yafang, H and Notkins, AL.(2010). IA-2 modulates dopamine secretion in PC12 cells. *Mol Cell Endocrinol* **315**, 81-86 10.1016/j.mce.2009.09.023

Pereira, M, Birtele, M, Shrigley, S, Benitez, JA, Hedlund, E, Parmar, M and Ottosson, DR.(2017). Direct Reprogramming of Resident NG2 Glia into Neurons with Properties of Fast-Spiking Parvalbumin-Containing Interneurons. *Stem Cell Reports* **9**, 742-751 10.1016/j.stemcr.2017.07.023

Perez-Moreno, JJ, Espina-Zambrano, AG, Garcia-Calderon, CB and Estrada, B.(2017). Kon-tiki enhances PS2 integrin adhesion and localizes its ligand, Thrombospondin, in the myotendinous junction. *J Cell Sci* **130**, 950-962 10.1242/jcs.197459

Peron, S and Berninger, B.(2015). Reawakening the sleeping beauty in the adult brain: neurogenesis from parenchymal glia. *Curr Opin Genet Dev* **34**, 46-53 10.1016/j.gde.2015.07.004

Piccin, D, Yu, F and Morshead, CM.(2013). Notch signaling imparts and preserves neural stem characteristics in the adult brain. *Stem Cells Dev* **22**, 1541-1550 10.1089/scd.2012.0390

Sakry, D, Neitz, A, Singh, J, Frischknecht, R, Marongiu, D, Biname, F, Perera, SS, Endres, K, Lutz, B, Radyushkin, K, Trotter, J and Mittmann, T.(2014). Oligodendrocyte precursor cells modulate the neuronal network by activity-dependent ectodomain cleavage of glial NG2. *PLoS Biol* **12**, e1001993
10.1371/journal.pbio.1001993

Sakry, D and Trotter, J.(2016). The role of the NG2 proteoglycan in OPC and CNS network function. *Brain Res* **1638**, 161-166 10.1016/j.brainres.2015.06.003

Sakry, D, Yigit, H, Dimou, L and Trotter, J.(2015). Oligodendrocyte precursor cells synthesize neuromodulatory factors. *PLoS One* **10**, e0127222 10.1371/journal.pone.0127222

San-Juan, BP and Baonza, A.(2011). The bHLH factor deadpan is a direct target of Notch signaling and regulates neuroblast self-renewal in *Drosophila*. *Dev Biol* **352**, 70-82 10.1016/j.ydbio.2011.01.019

Schnorrer, F, Kalchauer, I and Dickson, BJ.(2007). The transmembrane protein Kon-tiki couples to Dgrip to mediate myotube targeting in *Drosophila*. *Dev Cell* **12**, 751-766 10.1016/j.devcel.2007.02.017

Shtaya, A, Sadek, AR, Zaben, M, Seifert, G, Pringle, A, Steinhauser, C and Gray, WP.(2018). AMPA receptors and seizures mediate hippocampal radial glia-like stem cell proliferation. *Glia* **66**, 2397-2413 10.1002/glia.23479

Siegrist, SE, Haque, NS, Chen, CH, Hay, BA and Hariharan, IK.(2010). Inactivation of both Foxo and reaper promotes long-term adult neurogenesis in *Drosophila*. *Curr Biol* **20**, 643-648 10.1016/j.cub.2010.01.060

Simoës, AR and Rhiner, C.(2017). A Cold-Blooded View on Adult Neurogenesis. *Front Neurosci* **11**, 327 10.3389/fnins.2017.00327

Song, Y, Ori-Mckenney, KM, Zheng, Y, Han, C, Jan, LY and Jan, YN.(2012). Regeneration of *Drosophila* sensory neuron axons and dendrites is regulated by the Akt pathway involving Pten and microRNA bantam. *Genes Dev* **26**, 1612-1625 10.1101/gad.193243.112

Sousa-Nunes, R, Cheng, LY and Gould, AP.(2010). Regulating neural proliferation in the *Drosophila* CNS. *Curr Opin Neurobiol* **20**, 50-57 10.1016/j.conb.2009.12.005

Sousa-Nunes, R, Yee, LL and Gould, AP.(2011). Fat cells reactivate quiescent neuroblasts via TOR and glial insulin relays in *Drosophila*. *Nature* **471**, 508-512 10.1038/nature09867

Sun, W, Matthews, EA, Nicolas, V, Schoch, S and Dietrich, D.(2016). NG2 glial cells integrate synaptic input in global and dendritic calcium signals. *Elife* **5**, 10.7554/eLife.16262

Tanaka, EM and Ferretti, P.(2009). Considering the evolution of regeneration in the central nervous system. *Nat Rev Neurosci* **10**, 713-723 10.1038/nrn2707

Torper, O, Ottosson, DR, Pereira, M, Lau, S, Cardoso, T, Grealish, S and Parmar, M.(2015). In Vivo Reprogramming of Striatal NG2 Glia into Functional Neurons that Integrate into Local Host Circuitry. *Cell Rep* **12**, 474-481 10.1016/j.celrep.2015.06.040

Vaessin, H, Grell, E, Wolff, E, Bier, E, Jan, LY and Jan, YN.(1991). prospero is expressed in neuronal precursors and encodes a nuclear protein that is involved in the control of axonal outgrowth in *Drosophila*. *Cell* **67**, 941-953

Valny, M, Honsa, P, Kriska, J and Anderova, M.(2017). Multipotency and therapeutic potential of NG2 cells. *Biochem Pharmacol* **141**, 42-55 10.1016/j.bcp.2017.05.008

Van Der Heide, LP, Ramakers, GM and Smidt, MP.(2006). Insulin signaling in the central nervous system: learning to survive. *Prog Neurobiol* **79**, 205-221 10.1016/j.pneurobio.2006.06.003

Vigano, F and Dimou, L.(2016). The heterogeneous nature of NG2-glia. *Brain Res* **1638**, 129-137 10.1016/j.brainres.2015.09.012

Wills, Z, Bateman, J, Korey, CA, Comer, A and Van Vactor, D.(1999). The tyrosine kinase Abl and its substrate enabled collaborate with the receptor phosphatase Dlar to control motor axon guidance. *Neuron* **22**, 301-312

Yamamoto, S, Nagao, M, Sugimori, M, Kosako, H, Nakatomi, H, Yamamoto, N, Takebayashi, H, Nabeshima, Y, Kitamura, T, Weinmaster, G, Nakamura, K and Nakafuku, M.(2001). Transcription factor expression and Notch-dependent regulation of neural progenitors in the adult rat spinal cord. *J Neurosci* **21**, 9814-9823 21/24/9814 [pii]

FIGURE LEGENDS

FIGURE 1 *ia-2* interacts genetically with *kon*, *Notch* and *pros*.

(A) Quantitative real-time PCR (qRT-PCR) showing that loss of *kon* function in glia caused over 2-fold increase in *ia-2* mRNA levels. *kon* LOF: heterozygous mutant together with *kon* RNAi in glia (*genotype: kon^{c452}/UASkonRNAi; repoGAL4/+*). One Way ANOVA $p < 0.0001$ (RNAi). Over-expression of *kon* marginally decreased *ia-2* mRNA levels. One Way ANOVA $p = 0.045$ (GOF). Post-hoc Dunnett's test multiple comparisons to control. N=4 replicates. **(B)** qRT-PCR showing that over-expression of *ia-2* in glia downregulated *kon* mRNA levels. Thus, *ia-2* represses *kon* expression. Left: Unpaired Student t-test with Welch correction $p = 0.457$. Right: One Way ANOVA $p < 0.045$, post-hoc Dunnett's test multiple comparisons to control. N=4-6 replicates. **(C)** *ia-2* is functionally related to Notch: qRT-PCR showing that *ia-2* mRNA levels increased in *N^{ts}* mutant larvae at the restrictive temperature of 25°C. Unpaired Student t-test with Welch correction Left: $p = 0.4123$; Right: $p = 0.2182$. N=3 replicates. **(D)** *ia-2* is functionally related to *pros*: qRT-PCR showing that over-expression of *pros* in glia increased *ia-2* mRNA levels by 2 fold. Unpaired Student t-test with Welch correction. Left: $p = 0.1368$; Right: $p = 0.0428$. N=3 replicates. **(E)** qRT-PCR showing that *ia-2* RNAi knock-down in neurons lowered *ia-2* mRNA levels to 20%, whereas in glia it has no effect, meaning that *ia-2* is expressed in neurons. One Way ANOVA $p = 0.0004$, post-hoc multiple comparisons to control Dunnett's test. N=3 replicates. **(G,H,I)** Fusion protein *ia-2*-YFP revealed expression exclusively in neurons, as all *ia-2*-YFP+ cells were also *Elav*+, but *Repo*⁻ and *Dpn*⁻. N=4-16 larval VNCs. **(F)** Illustration to show that *kon* and *ia-2* functions are restricted to glia and neurons, respectively, and they repress each other. (G, horizontal views; H, transverse view; I, higher magnification view). With more than two sample types, asterisks

indicate multiple comparison post-hoc tests to controls: * $p < 0.05$, ** $p < 0.01$, *** $p < 0.001$,
**** $p < 0.0001$.

FIGURE 2 *ia-2* influences neural cell fate stability. **(A,B)** Loss of *kon* function in glia (*kon^{c452}/UASkonRNAi; repoGAL4/+*) increased the number of *ia-2*-YFP+ cells along the midline. One Way ANOVA $p < 0.0001$, post-hoc Tukey's test. N=5-8 VNCs. **(C)** The ectopic *ia-2*-YFP+ cells in *kon* loss of function were not Repo+ glia. N=7 VNCs. **(D, E)** Neither loss nor gain of *ia-2* function affected number of Eve+ neurons. One Way ANOVA $p = 0.2277$. N=7-12 VNCs. **(F,G)** Loss of *ia-2* functions (*elavGAL4>UASia-2RNAi*) increased Pros+ cell number. One Way ANOVA $p = 0.0002$, post-hoc Dunnett's test. N=8-10 VNCs. **(H)** Loss of *ia-2* function (*Df(2L)ED7733/+; elavGAL4>UASia-2RNAi*) caused VNC overgrowth. **(I,J)** Both loss and gain of *ia-2* function increased Dpn+ cell number. One Way ANOVA $p = 0.0021$, post-hoc Dunnett. N=7-12. Asterisks indicate multiple comparison post-hoc tests to a fixed control: * $p < 0.05$, ** $p < 0.01$, *** $p < 0.001$, **** $p < 0.0001$.

FIGURE 3 Injury induced *ia-2* expression and neurogenesis. **(A-D)** Crush injury in the larval abdominal VNC carried out at 74-76h after egg laying (AEL) caused: **(B,D)** formation of multiple ectopic Dpn+ neural stem cells (arrowheads) by 5-7 hours post-injury (N=6/17 VNCs). Dpn+ cells were *ia-2*-YFP⁻; and **(C)** an increase in the levels of *ia-2* mRNA at 5-7h post-injury, which recovered homeostatically by 24h, detected by qRT-PCR. N=3 replicates. **(E,G,H)** Crush injury in the larval abdominal VNC at 96h AEL caused ectopic Dpn+ cells by 6 hours post-injury (arrowheads). Most Dpn+ cells were *ia-2*-YFP⁻, but some were *ia-2*-YFP⁺. N=4/9 VNCs. **(H)** There were ectopic Dpn+ cells dorsally, on the edge of the neuropile. **(I,J)** Crush injury in the larval abdominal VNC at 117h AEL caused ectopic Dpn+ cells by 12 hours post-injury (arrowheads). Dpn+ cells were found in ectopic dorsal positions devoid of developmental neural stem cells (arrowheads in J). N=9/32 VNCs. **(B,G,I)** Horizontal views, **(H,J)** sagittal views and **(D,J)** transverse views.

FIGURE 4 **la-2 and Kon regulate *dilp-6* expression in neurons and glia, respectively. (A,B)** *Dilp-6GAL4>UAShisYFP* cells are mostly Repo⁺ glia (arrows), and Pros⁻, meaning they are not astrocyte-like glia surrounding the neuropile, as seen in transverse views in (B); from position they appear to be cortex and surface glia. Some cells are Repo⁻ (arrowheads, left column) and Elav⁺ (arrows, right column) meaning they are neurons. **(C,D)** *inr* expression visualized with reporter *InR^{NP2552}GAL4>UAShistoneYFP* is expressed in some Repo⁺ neuropile glia and in some in Elav⁺ neurons. **(E-H)** qRT-PCRs showing that: **(E,F)** *ia-2* knock-down in neurons (*elavGAL4>UASia-2RNAi*) downregulates *dilp-6* mRNA levels, and over-expression of *ia-2* (with *UAS-ia-2^{GS11438}*) up-regulates *dpn*, *dilp-6* and *elav* mRNA. **(E)** Unpaired Student-t tests comparing effect on each gene separately, differences not significant; **(F)** One Way ANOVA per gene group, not significantly different. N=4 replicates for both. **(G,H)** *kon* knock-down in glia (*kon^{c452}/UASKonRNAi; repoGAL4/+*) downregulates *dilp-6* mRNA levels, whereas over-expression on *kon* does not have a remarkable effect. N=3 replicates for both. **(G)** One Way ANOVA per gene group, only differences in *dilp-6* mRNA significant p=0.0362. One Way ANOVA per gene group, not significantly different. *p<0.05.

FIGURE 5 **la-2, Kon and Dilp-6 are linked through a neuron-glia communication loop. (A)** Over-expressed HA-tagged Kon^{ICD} in glia (*repoGAL4>UASKon^{ICD}::HA*) visualized in stage 16 embryos with anti-HA antibodies, localizes to glial nuclei (arrowheads). **(B,C)** Over-expression of either the intracellular domain of either *kon* (*kon^{ICD}*) or *dilp-6* is sufficient to increase glial cell number (visualized with *repoGAL4>UAShistone-YFP*). Over-expression of a dominant negative form of the insulin receptor rescues the increase in cell number caused by *dilp-6* (*repo>hisYFP, dilp-6, InRDN*), meaning that autocrine InR signaling regulates glial proliferation. One Way ANOVA p<0.0001, post-hoc Tukey's test multiple comparisons between all samples. N=15-28 VNCs. **(D,E)** *kon-RNAi* knock-down in neural stem cells with *insecGAL4* does not affect Dpn⁺ expression or cell number. Unpaired Student t-test, p=0.3111. N=10 VNCs **(F)** Illustration summarising that a positive feedback autocrine

loop involving Dilp-6, InR and Kon promotes both glial proliferation and Dilp-6 production. Asterisks refer to multiple comparison post-hoc test, all samples vs. all: ** $p < 0.01$, **** $p < 0.0001$.

FIGURE 6 **ia-2 and Dilp-6 induce ectopic neural stem cells that do not express ia-2 and result from InR signaling in glia. (A-D)** Over-expression of *ia-2* and *dilp-6*, but not *kon-full-length*, increased Dpn+ cell number. Both *ia-2* and Dilp-6 induced Dpn+ at the midline and in lateral positions: here showing *ia-2* induction most prominently along the midline (arrowheads), and *dilp-6* in lateral positions around neuropile (arrowheads; arrows indicate midline Dpn+ cells in C). **(B)** Ectopic Dpn+ cells did not express *ia-2*-YFP (arrowheads). **(D)** Genetic epistasis analysis showing that: the increase in Dpn+ cell number caused by *ia-2* over-expression was rescued by *dilp-6 RNAi* and *kon-RNAi* knock-down in glia, meaning that *ia-2* increases Dpn+ cells via glial Kon and Dilp-6; and preventing insulin signaling with InR^{DN} in glia rescues the increase in Dpn+ cell number caused by *dilp-6* over-expression, meaning that ectopic Dpn+ originate from InR signaling in glia. One Way ANOVA $p < 0.0001$, post-hoc Tukey's test multiple comparisons all samples vs. all. N=8-13 VNCs. **(E)** Illustration of neuropile glia conversion to Dpn+ cells. **(A)** Horizontal views; **(B)** higher magnification; **(C)** transverse views. Asterisks refer to multiple comparison post-hoc tests: * $p < 0.05$, *** $p < 0.0001$, **** $p < 0.0001$.

FIGURE 7 **Ectopic neural stem cells originate from glia. (A,B)** Over-expression of *dilp-6* induced Dpn expression in Repo+ neuropile glial cells (arrowheads). N= 10 VNCs. **(C,D)** G-TRACE expression in glia with *repoGAL4* revealed GFP+ cells that were glial cells from cell lineage's origin, and RFP+ newly generated glial cells. Dpn colocalised in neuropile glia with both GFP and RFP, meaning that Dpn+ cells originated from glia, and at that point in time these cells still retained glial features. N= 8 VNCs. **(A,C)** horizontal, and **(B,D)** transverse views.

FIGURE 8 Injury-induced neurogenesis is triggered by a neuron-glia communication loop

involving insuling signalling and Kon. (A,C) In the abdominal larval VNC, neurons express *ia-2*, and glia express *kon* at very low levels. Neuropile NG2-like glia have active Notch and Pros. In the normal, uninjured abdominal VNC, *InR* is expressed by glial cells and neurons; *ia-2* expression is maintained in neurons, *kon* and *dilp-6* are switched off, and there are no neural stem cells (NBs). **(B)** Injury to the abdominal VNC provokes a dramatic surge in *ia-2* and in *kon* mRNA levels. This drives the initial secretion of Dilp-6 from a small group of neurons. Secreted Dilp-6 binds InR in glia, and InR signaling may facilitate cleavage and activation of Kon. Kon^{ICD} activates glial proliferation and expression of *dilp-6* in glia. Secreted Dilp6 binds InR in cortex/surface glia, boosting a positive feedback loop that amplifies Dilp-6 production from non-neuropile glia. In Notch+ Pros+ NG-2-like glia surrounding the neuropile, Dilp-6 and InR signaling cause the Kon-dependent up-regulation of Dpn+. Dpn+ neural stem cells could potentially thereafter result in the production of new neurons and glia. The production of Dpn+ cells in glia depends on Kon, but Kon-full length alone is not able to induce *dpn* expression or new Dpn+ cells. Thus, neurogenesis requires insulin signaling and Kon downstream. Together, *ia-2*, Dilp-6, InR and Kon can induce neurogenesis and gliogenesis, matching cell populations during regeneration.

Supplementary Figure 1 Modifier genetic screens to identify genes interacting with *kon*

(A,B) Over-expression of *kon* in glia with *repoGAL4* (*repo>UASFlyBow*, *UASKon-full-length*) caused a phenotype of very long ventral nerve cord (A), and in neurons with *elavGAL4* too, although to a lesser extent **(B)**. These phenotypes were quantified by using the reporter *UASFlyBow*, and the VNC measured using ImageJ tools. RNAi knock-down of candidate genes can rescue these phenotypes, some examples are shown here. **(C-G)** The *kon* gain of function (GOF) phenotype resulting from over-expressing *kon-full-length* in either neurons or glia, can be rescued by RNAi knock-down of: **(C)** predicted interactors of Kon or NG2, most prominently in glia; Kruskal Wallis ANOVA $p < 0.0001$, post-hoc Dunn test to *>FlyBow*, *kon* controls. N=4-24 VNCs. **(D)** α and γ -secretases that cleave NG2 and

Notch, from glia. ; Kruskal Wallis ANOVA $p < 0.0001$, post-hoc Dunn test to *>FlyBow, kon controls*.

N=4-24 VNCs. **(E)** known Kon partners, e.g. integrins, and other transmembrane proteins, also from neurons; ; Kruskal Wallis ANOVA $p < 0.0001$, post-hoc Dunn test to *>FlyBow, kon controls*. N=3-24

VNCs. **(F)** cytoplasmic phosphatases, from either glia or neurons; Kruskal Wallis ANOVA $p < 0.0001$, post-hoc Dunn test to *>FlyBow, kon controls*. N=7-24 VNCs. VNC length indicated in yellow in (A,B).

*Asterisks indicate multiple comparison post-hoc tests to controls: * $p < 0.05$, ** $p < 0.01$, *** $p < 0.001$, **** $p < 0.0001$.

Supplementary Figure 2 Modifier candidate genetic screens identify genes encoding

transmembrane phosphatases and insulin signaling factors as interacting with *kon*. (A,B) Over-

expression of *kon* in glia causes a very long VNC **(A)**, and in neurons too, but to a lesser extent **(B)**.

RNAi knock-down of candidate genes can rescue these gain of function phenotypes, some examples are given. **(C,D)** Quantification of normalized VNC length shows rescue prominently by most

transmembrane phosphatases, the Notch-related *Akap200*, and genes functionally related to the

insulin signaling pathway, and including *Akt*, *lar* and *ia-2*. Normalised measurements are given as a

ratio of the VNC over total larval length. Kruskal-Wallis ANOVA $p < 0.0001$, post-hoc Dunn's test

comparison to controls *repo>kon* or *elav>kon*. **(C)** N=2-28; **(D)** N=2-31. *Asterisks indicate multiple

comparison post-hoc tests to controls: * $p < 0.05$, ** $p < 0.01$, *** $p < 0.001$, **** $p < 0.0001$.

Supplementary Figure 3 Loss and gain of *kon* function prominently affected *ia-2* expression.

(A,B) Exploratory quantitative real-time PCR (qRT-PCR), N=2 replicates each: **(A)** showing the change

in mRNA levels for candidate genes upon *kon* RNAi targeted to either neurons (with *elavGAL4*) or glia (with *repoGAL4*). *ia-2* mRNA levels increased at least 3 fold when *kon* was knocked-down in glia; **(B)**

showing the effect of *kon* gain of function. *kon* over-expression in either neurons or glia decreased

ia-2 mRNA levels. The first two columns have been left cut out as they are controls with the increase

in *kon* mRNA with *kon* over-expression, which are very high compared to the rest. **(C,D)** Further

replicates were carried out for a selected group of genes, and they validate that *kon* prominently regulates *ia-2* expression. N=4 replicates each. The first columns represent the very high increase in *kon* mRNA with *kon* over-expression, and they have been cut as they go well beyond this scale compared to the rest.

Supplementary Figure 4 Alterations in *ia-2* levels cause no obvious neuronal phenotypes.

(A) Neurons and their axonal fascicles are visualised with anti-FasII. N=7-11 VNCs. **(B)** Neurons and their dendrites are visualized with anti-BP102. N=9-10 VNCs. No abnormal phenotypes were observed.

Figure 1 *ia-2* interacts genetically with *kon*, *Notch* and *pros*

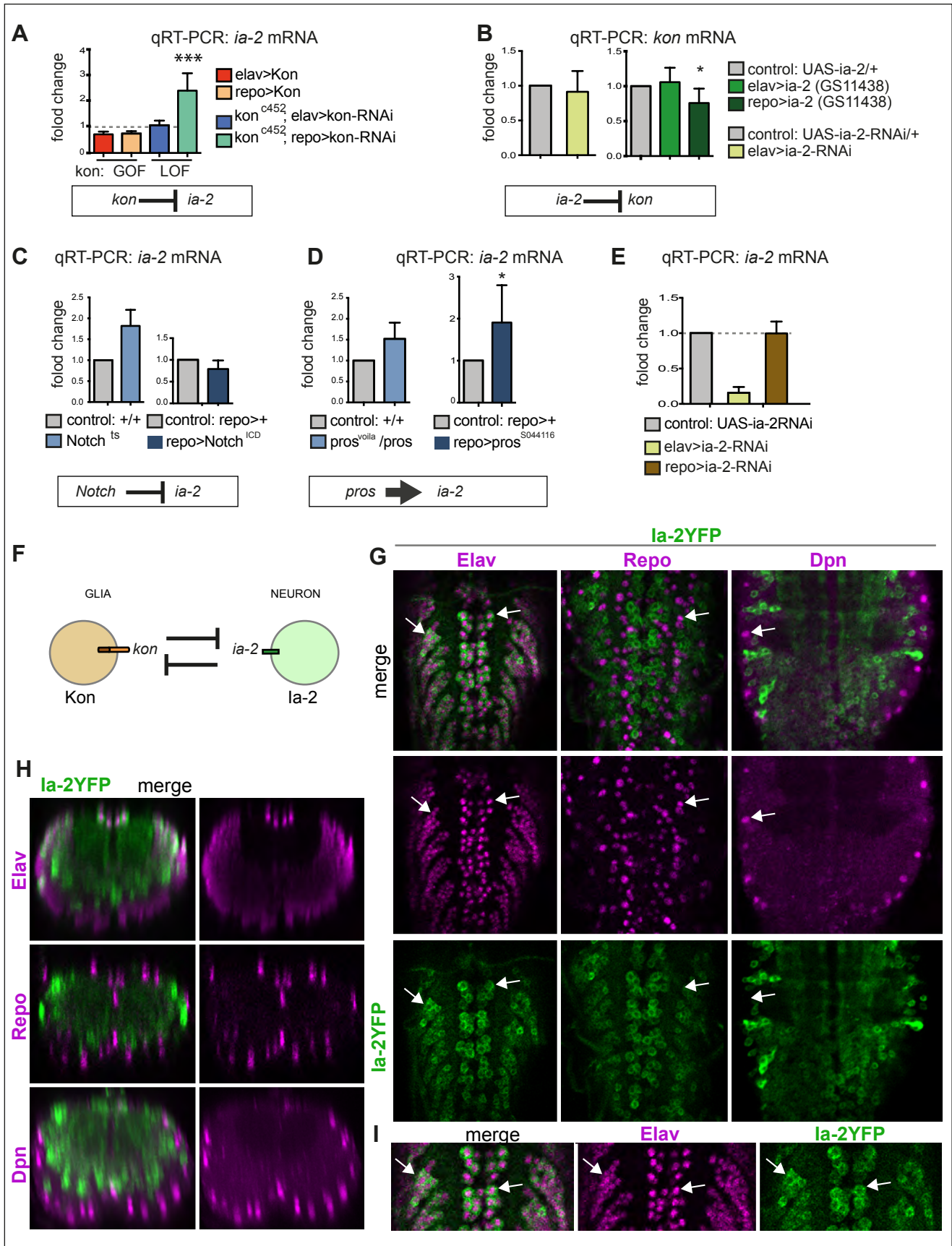


Figure 2 *ia-2* influences neural cell fate stability

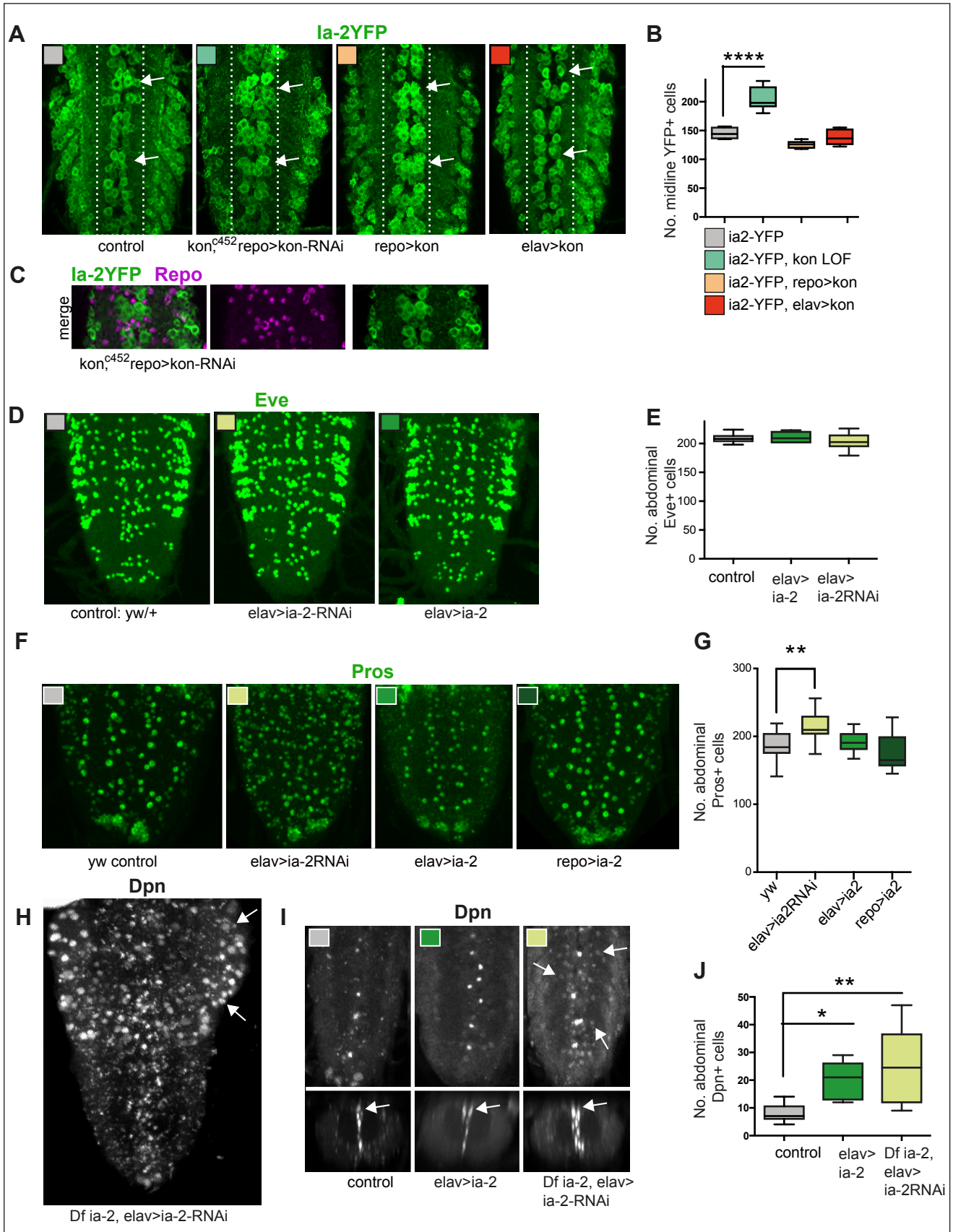


Figure 3 Injury induces *ia-2* expression and neurogenesis

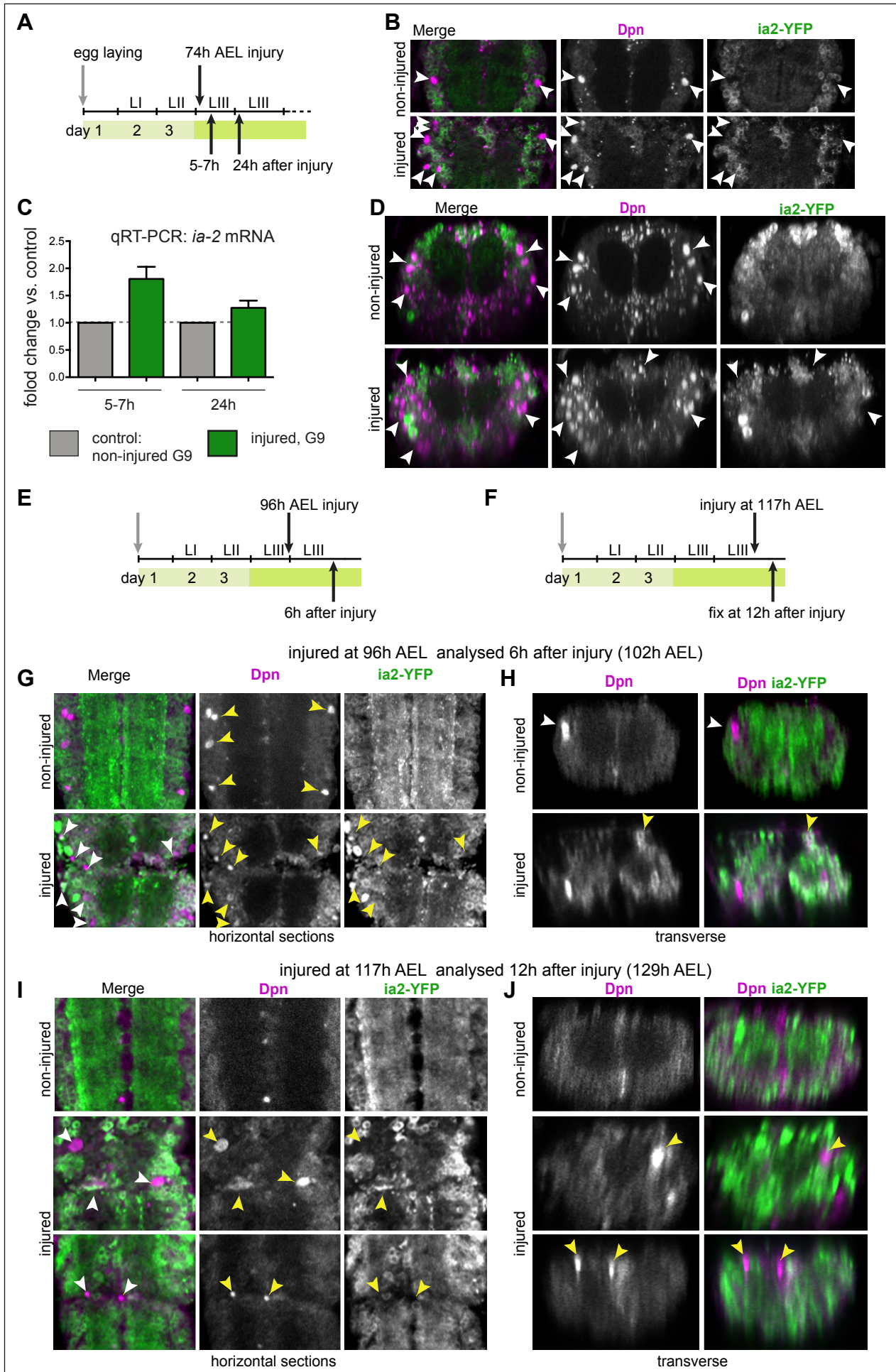


Figure 4 *la-2* and *Kon* regulate *dilp-6* expression in neurons and glia, respectively

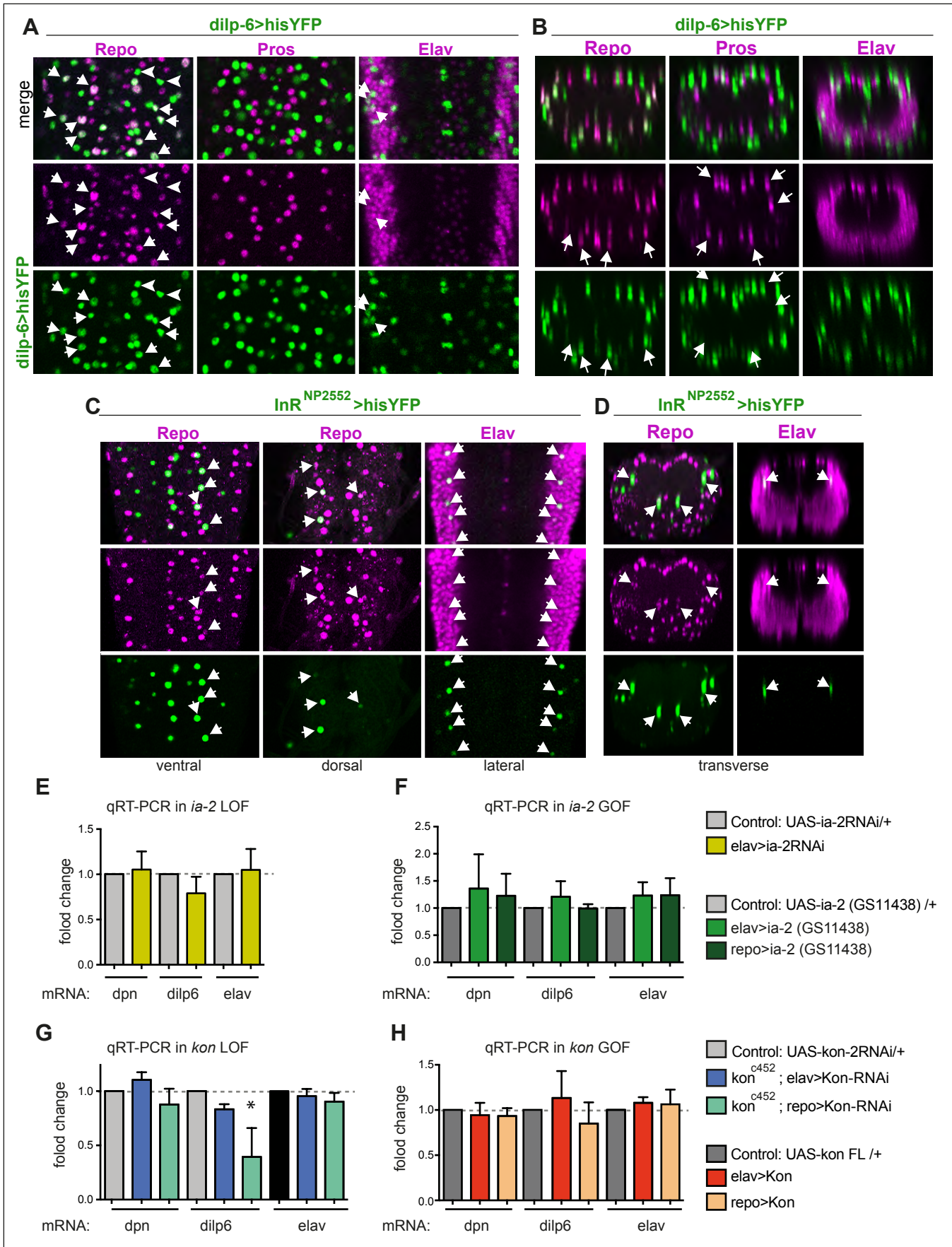


Figure 5 Ia-2, Kon and Dilp-6 are linked through a neuron-glia communication loop.

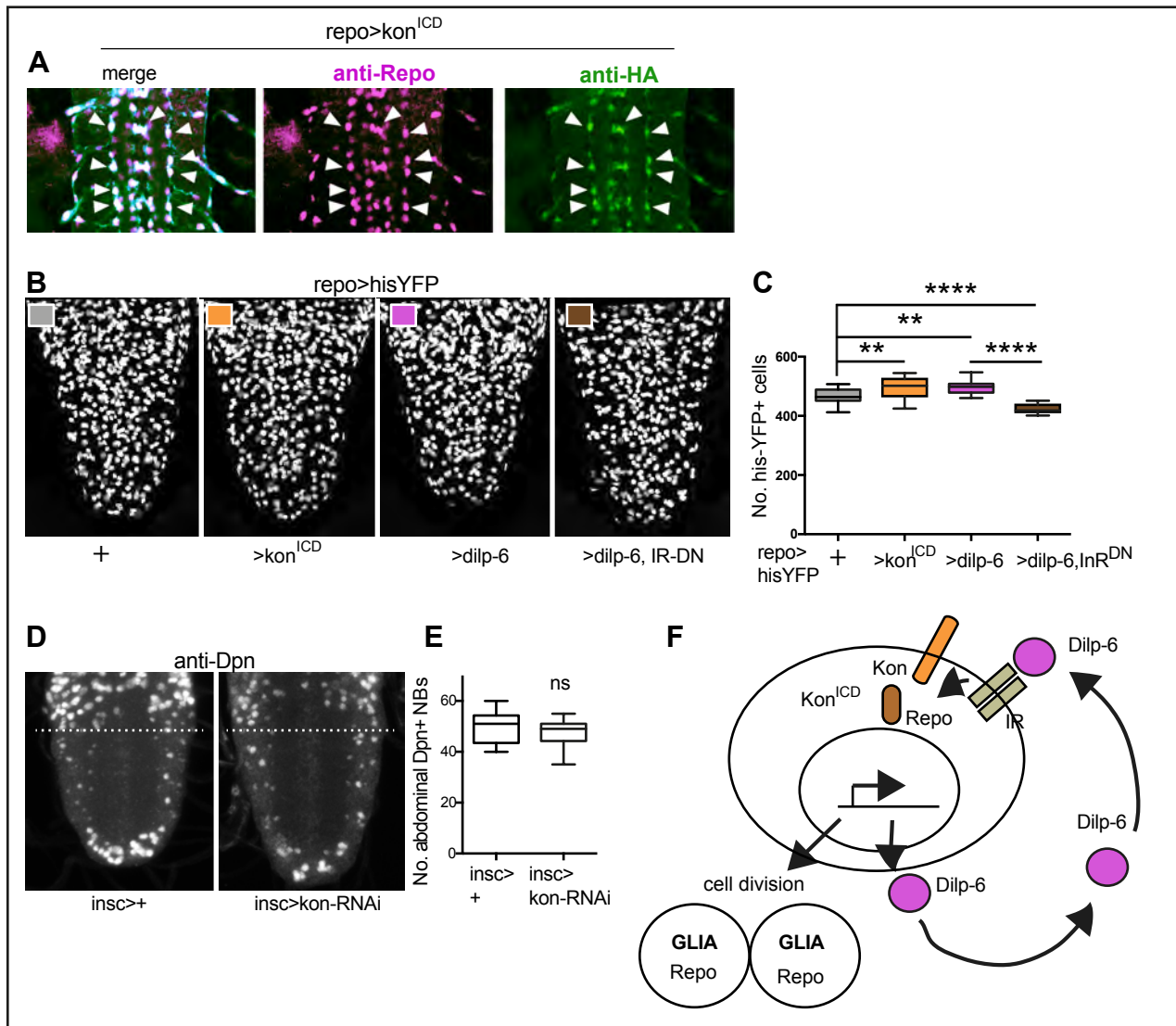


Figure 6 *ia-2* and Dilp-6 induce ectopic neural stem cells that do not express *ia-2* and result from InR signaling in glia.

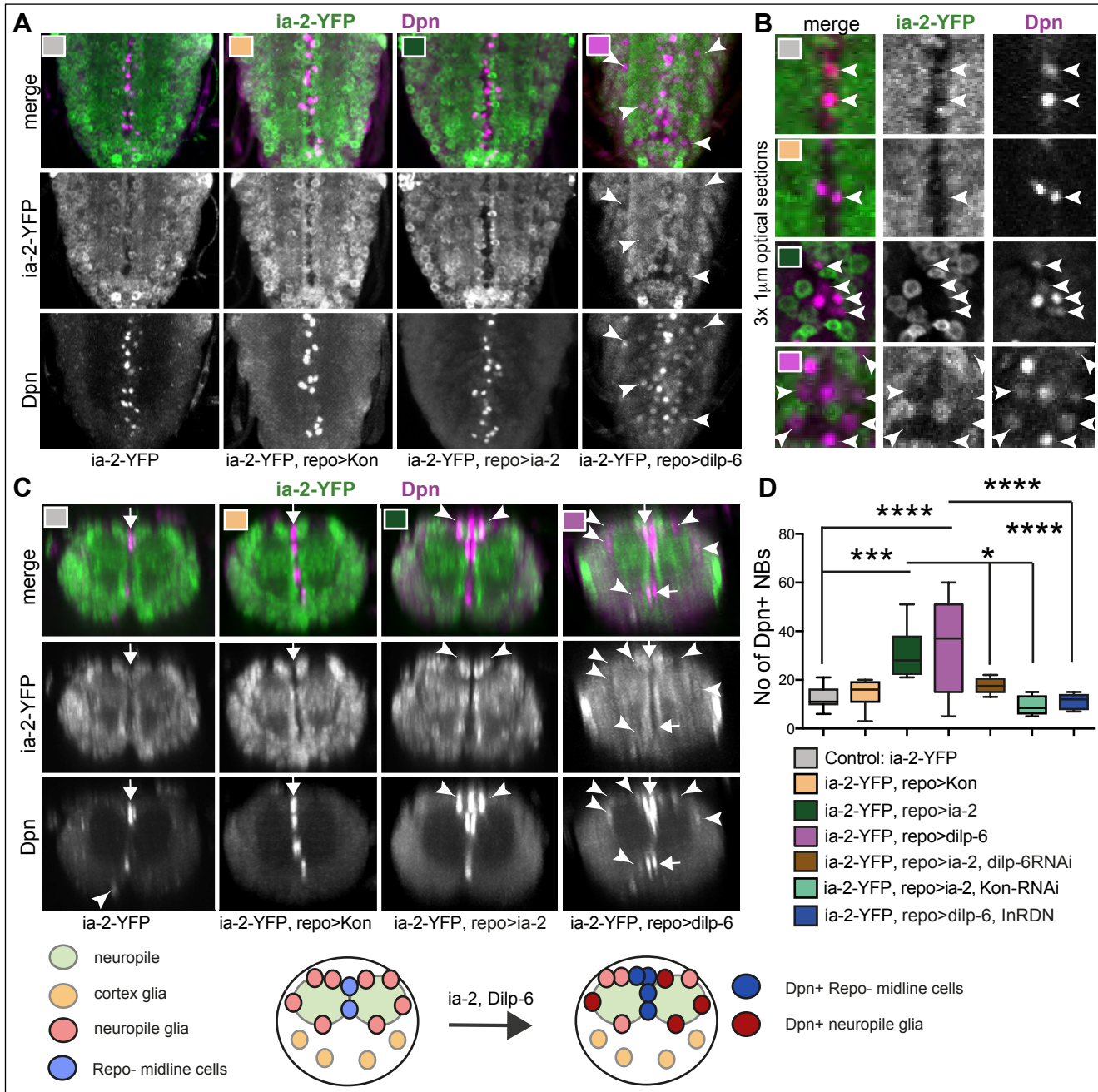


Figure 7 Ectopic neural stem cells originate from glia

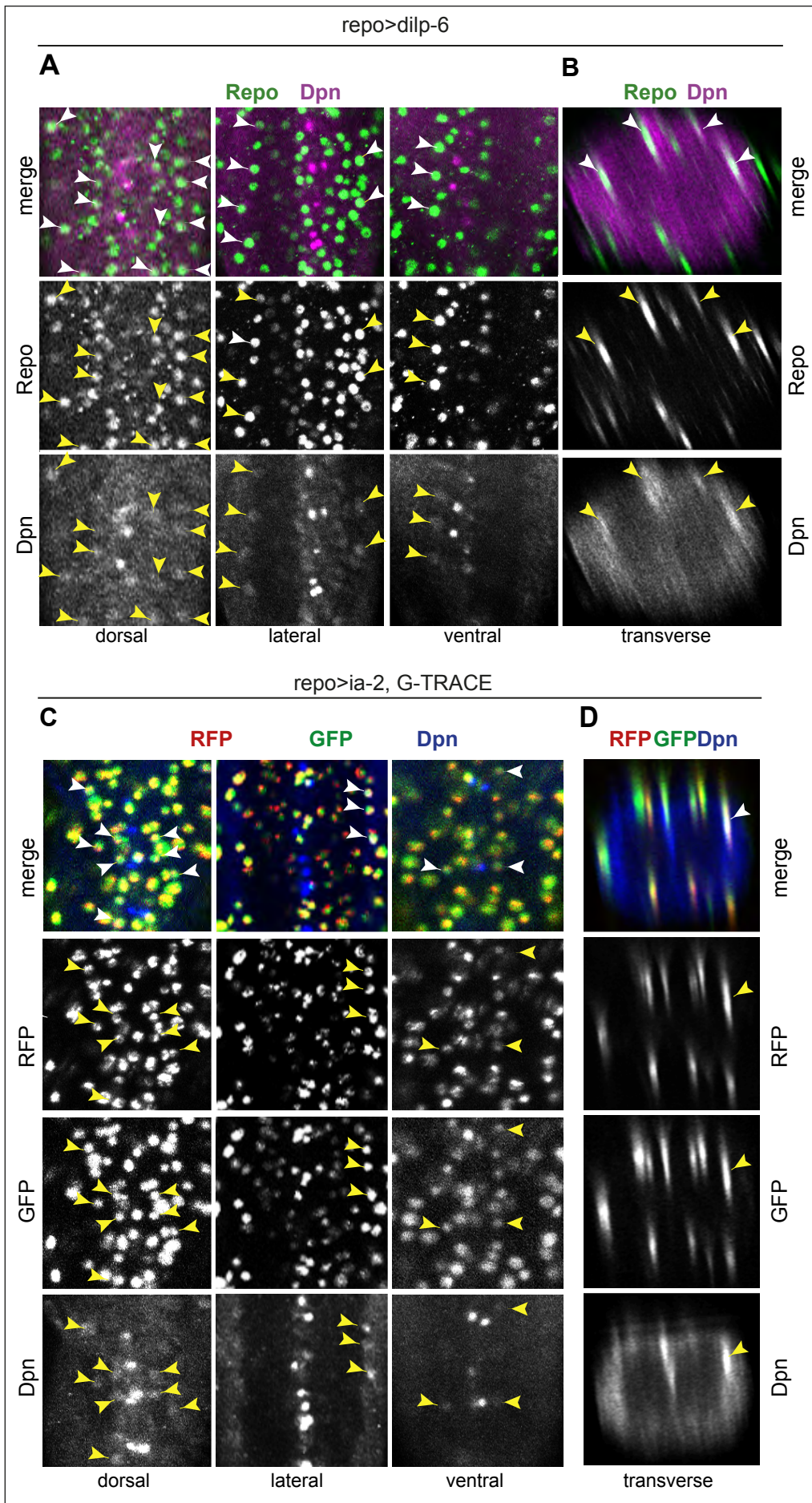
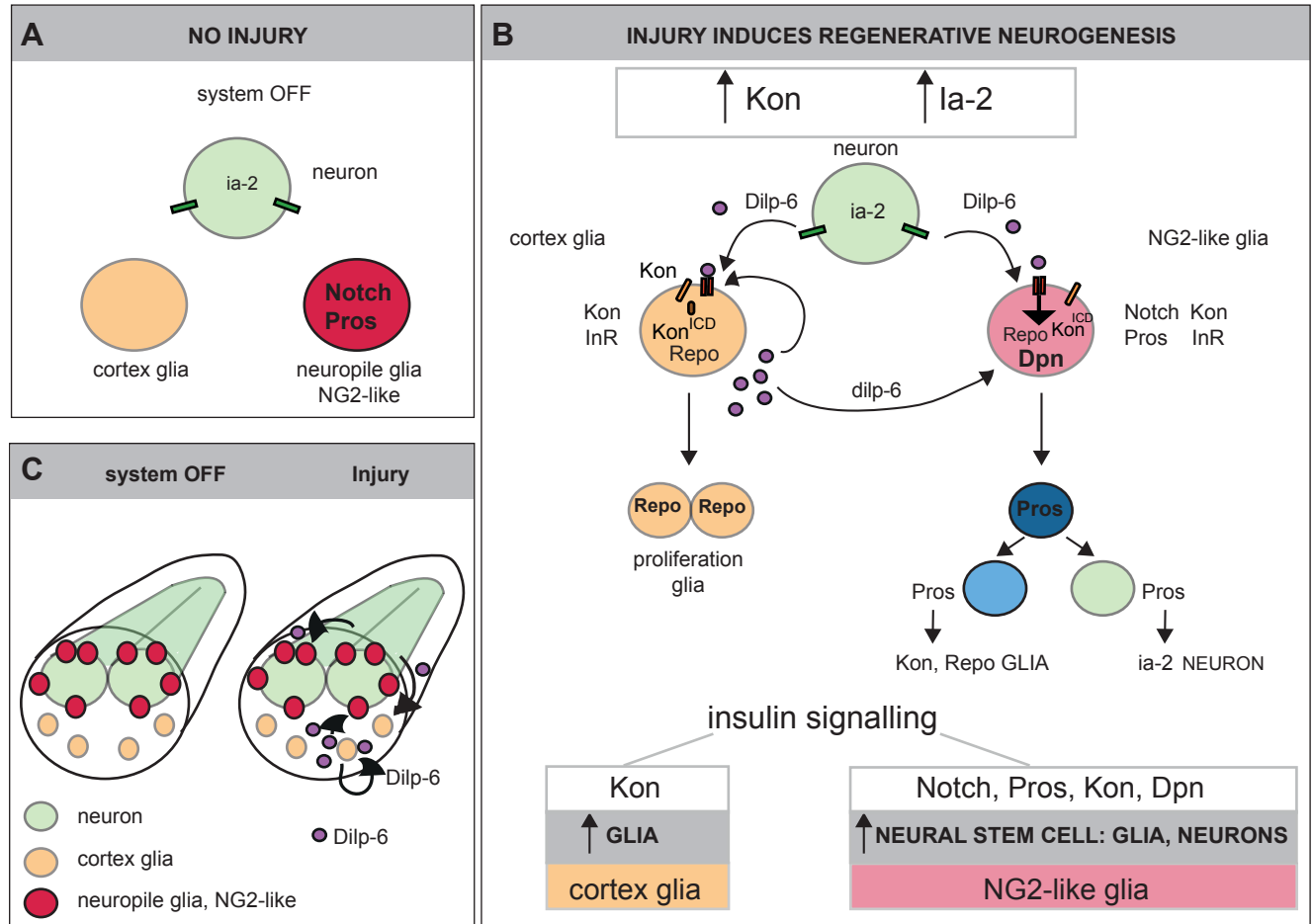
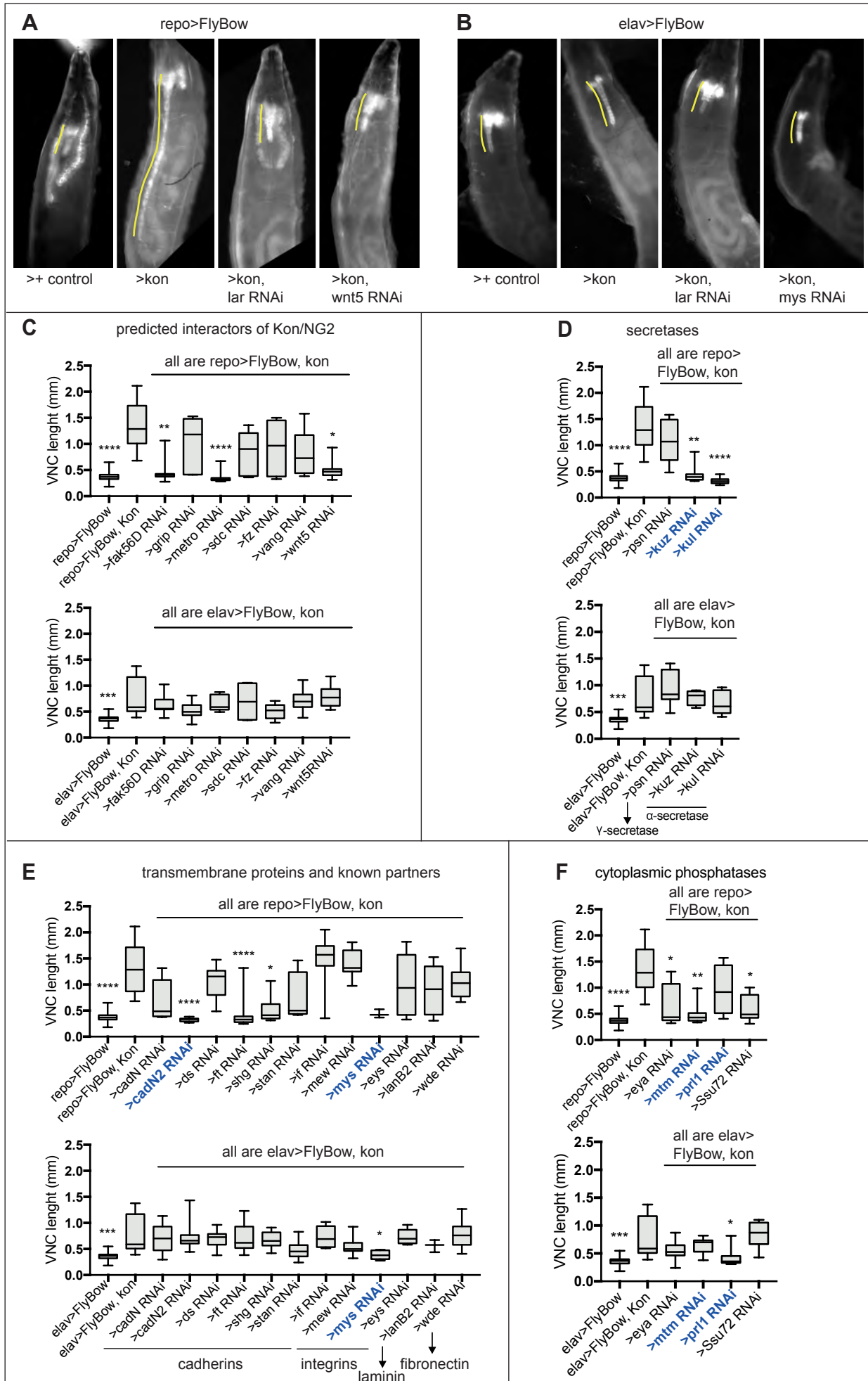


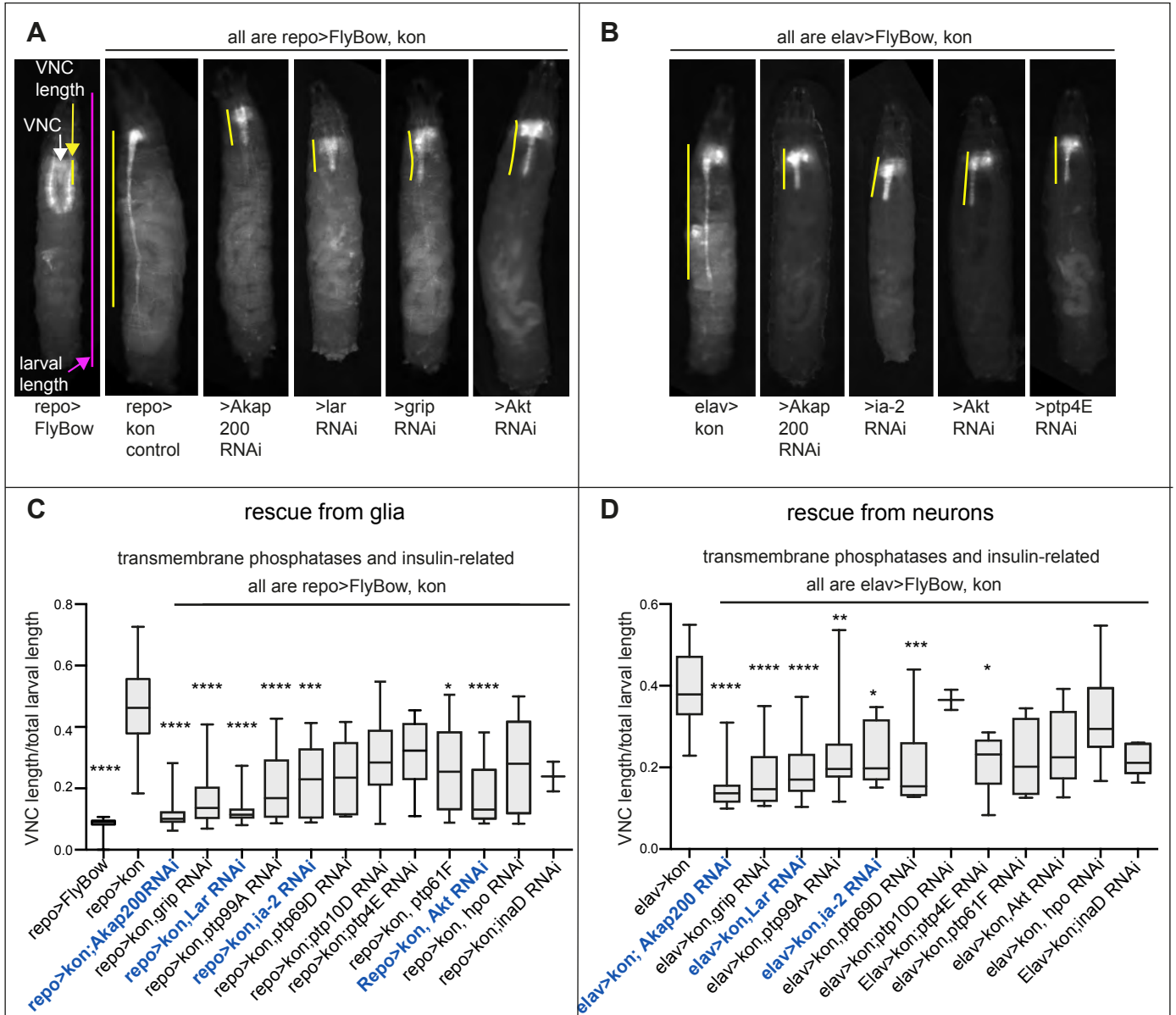
Figure 8 Injury-induced neurogenesis is triggered by a neuron-glia communication loop involving insulin signalling and Kon.



Supplementary Figure 1 Modifier genetic screens to identify genes interacting with *kon*

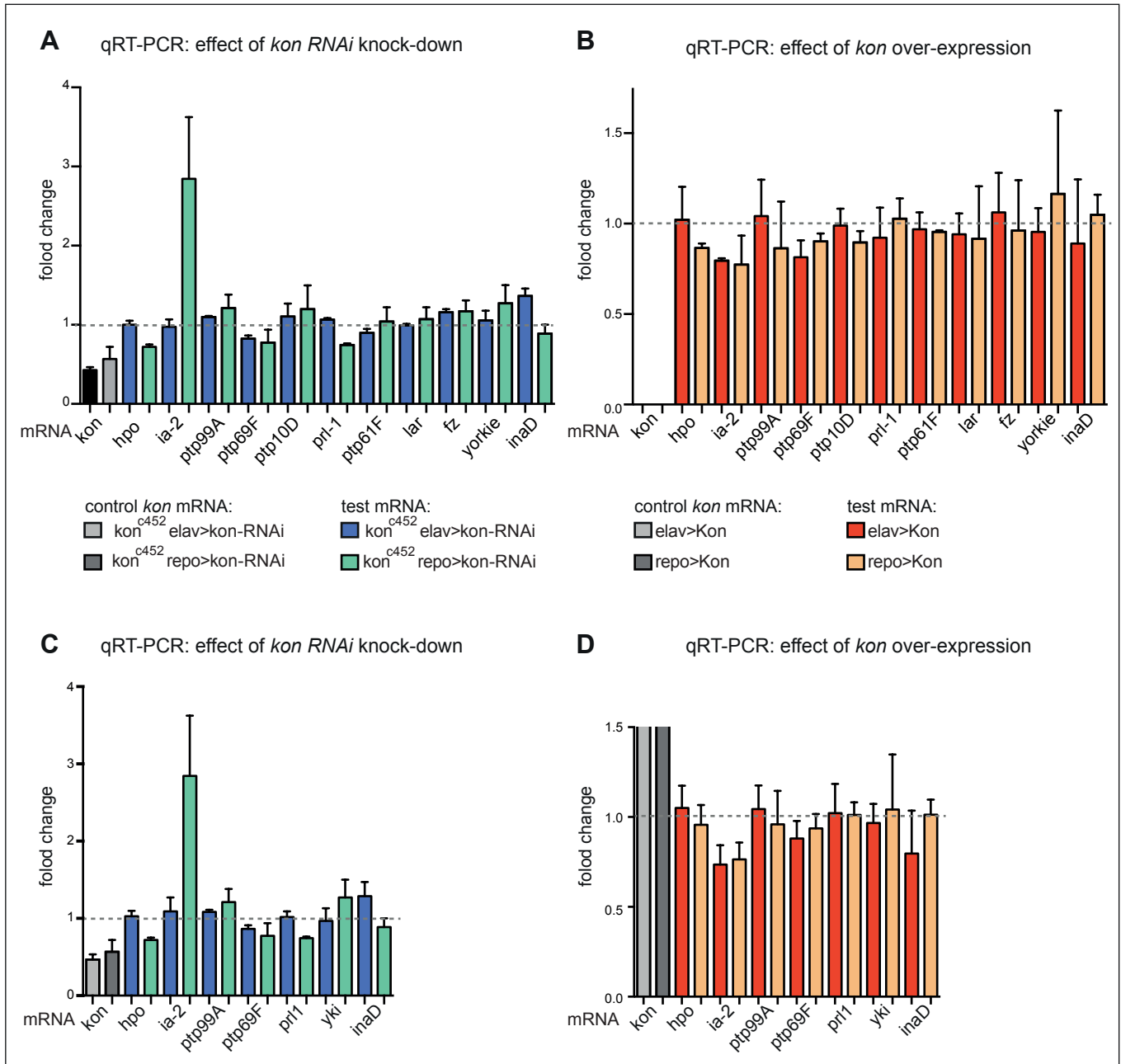


Supplementary Figure 2 Modifier candidate genetic screens identify genes encoding transmembrane phosphatases and insulin signaling factors as interacting with kon.



Supplementary Figure 3

Loss and gain of kon function prominently affects *ia-2* expression



Supplementary Figure 4 Alterations in *ia-2* levels cause no obvious neuronal phenotypes

